POLITECNICO DI TORINO

Department of Mechanical Engineering

Master's Degree Thesis

Structural FEM analysis of innovative sandwich configuration for automotive application

Supervisor

Prof. GIACOMO FRULLA

Company Tutor

NICOLA GIULIETTI

Candidate

EHSAN KHARRAZI

A.Y. 2019/2020

Abstract:

A sandwich structure (composite) consists of three main parts: two thin, stiff, and strong faces and a thick, light, and weaker core. The faces are adhesively bonded to the core to obtain a load transfer between the components. The basic advantage of sandwich structures (composite) is its high strength to weight ratio, high resistance to corrosion and impact, good insulation to acoustic and heat.

This thesis research is based on Madflex, an innovative technology in the field of sandwich that after receiving some changes in the core geometry, it enables this sandwich to be flexible, even rollable in one direction of bending and in the opposite side, it is totally rigid.

In this research, as the first step, we have performed the experimental test on different samples of Madflex in two different directions of flexural according to the ASTM D7250/D7250M Standard, then we have made a FEM model simulation of Madflex in the NASTRAN program and applied bending test to later compare the results with the experiment test performed in the laboratory. The feasibility of the Madflex application in the automotive section has also been investigated as a spoiler (wing) aerodynamic feature.

ACKNOWLEDGEMENTS

First of all, I would like to thank my supervisor Prof. GIACOMO FRULLA. He selflessly shared his knowledge and experiments and he always showed a great will to help me.

This thesis is done with the collaboration of CoRe Co. I would like to thank all of the company staff and particularly Mr. NICOLA GIULIETTI. They supported me with a wealth of knowledge and experience in the field of composite materials.

In the end, I would like to thank my parents and my family, who have supported me selflessly during my growing up and education.

Polytechnic of Turin, December 2020 EHSAN KHARRAZI

Table of Contents

List of Figures

List of Tables

1.1 Conventional Sandwich structure:

A sandwich consists of three main parts as illustrated in Figure 1.1 Two thin, stiff, and strong faces are separated by a thick, light, and weaker core. The faces are adhesively bonded to the core to obtain a load transfer between the components.

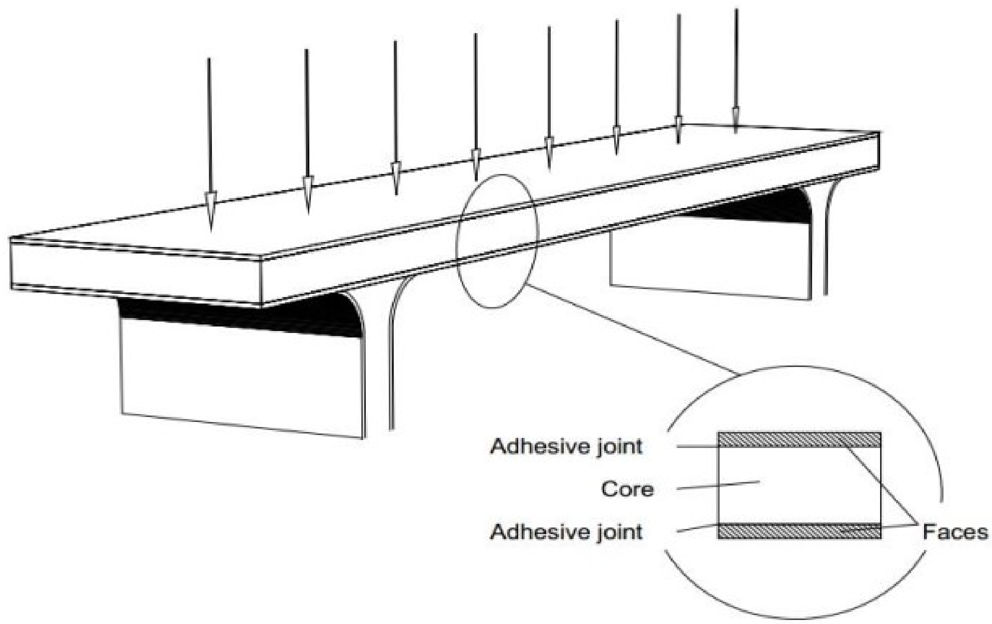

Figure 1.1 Conventional Sandwich structure

The operation of a sandwich is much the same as that of an I-beam, which is an efficient structural shape because as much as possible of the material is placed in the flanges situated farthest from the center of bending or neutral axis. Only enough material is left in the connecting web to make the flanges act in concert and to resist shear and buckling. In a sandwich the faces take the place of the flanges and the core takes the place of the web. The difference is that the core of a sandwich is of a different material from the faces and it is spread out as a continuous support for the faces rather than concentrated in a narrow web. The faces will act together to form an efficient stress couple or resisting moment counteracting the external bending moment. The core resists shear and stabilize the faces against buckling or wrinkling. The bond between the faces and the core must be strong enough to resist the shear and tensile stresses set up between them. The adhesive that bonds the faces to the core is thus of critical importance.

1.2 Madflex

Flexibility and stiffness on a single panel. This is what makes the MadFlex unique. In fact, thanks to its innovative mechanical features, you can have a panel that is flexible, even rollable, on the one side, while it is absolutely crushproof on the other. The MadFlex is a composite material panel, having a layered structure, particularly a sandwich-like structure.

It comprises two outer layers and an intermediate one. Of course, depending on the application to develop, CORE will choose the best geometry and the most suitable combination of materials to build the sandwich. The company has already tested a number of different solutions, using for example carbon fibers, Kevlar, aramidic fibers, foam and others, obtaining excellent results.

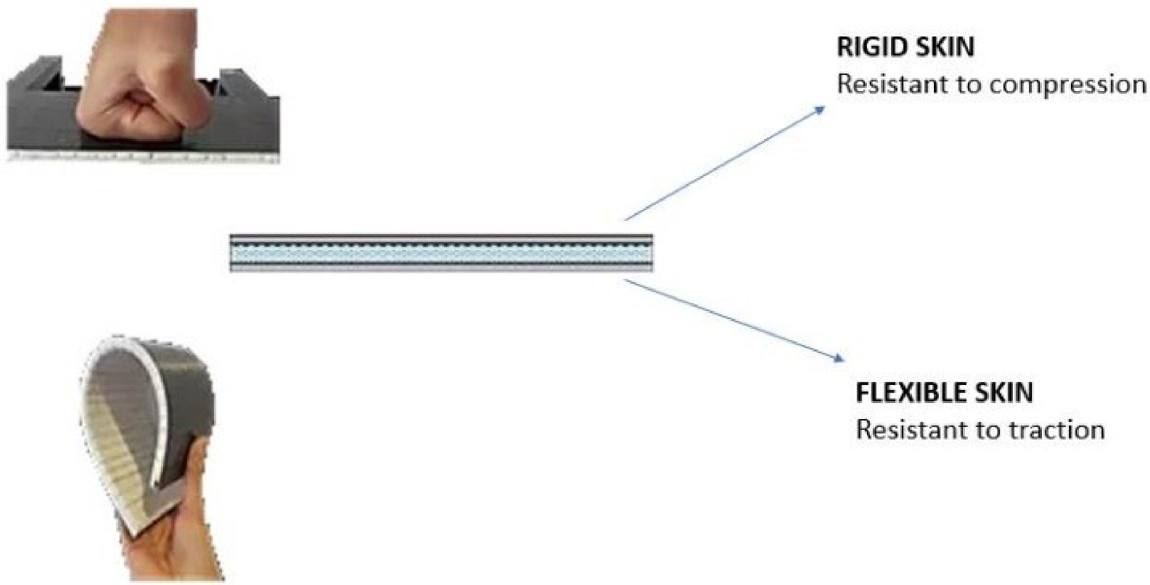

Figure 1.2 Madflex configuration

1.3 Madflex properties

- Low lightness
- Structure Strength
- Thermoformable
- Thermic insulating
- Temperature resistant
- Anti-seismic
- Easy to transport
- Thermal insulating
- Resistant to chemical agents
- Fireproof
- Biocompatible
- Endless surface finishing

The MadFlex can be applied to any industrial segment that is looking for lighter, safer, easier to modulate materials, with a lower environmental impact. Thanks to the infinite combinations of available materials and its extreme modularity, it can be used for both small components (e.g. interior car) and bigger and more complex ones (e.g. tensile structures)

	Bending stiffness rigid side	**Bending stiffness rollable side**	**Tensile strength**	**Flexural strength**	**Flatwise compressive strength**
	[N·m2/m]	[N·m2/m]	[kN/m]	[MPa]	[MPa]
TEST METHOD	ASTM D7250/D7250M	ASTM D7250/D7250M	ASTM D3039/D3039M	ASTM D7250/D7250M	ASTM C365/C365M
Max value configurations	250	2,0	700	450	2,4
Min value configurations	13	0,1	350	95	1,2

Table 1.1 MadFlex Mechanical Properties

1.4 Madflex Comparison with Other Material

The uniqueness of the MadFlex is that it combines the pros of existing fabrics (lightness, thinness, flexibility) with those of traditional materials (strength, rigidity, shear strength). However, comparing it with these would be limiting.

In fact, not only can the MadFlex replace existing fabrics and materials, but, given its mechanical features, it can also simplify entire projects by abolishing the use of cables, junctions and struts. Moreover, the MadFlex has intrinsic insulation abilities, which allow manufacturers to avoid additional layers, thus saving materials and labor. In order to create a proper prototype, CoRe will work alongside its customers to develop an engineering project that meets the required needs and represents excellence.

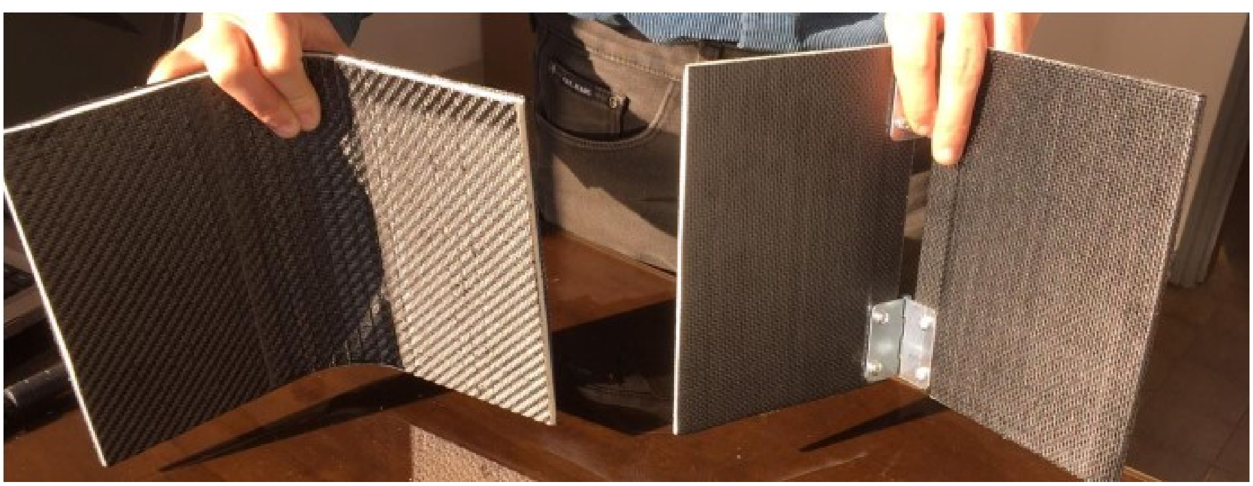

Figure 1.3 Sandwich with a hinge in MadFlex VS Sandwich with a mechanical hinge

Compared to **rigid structural materials**, as metals and polymers, with the same stiffness and mechanical
strength, the MadFlex presents the following advantages:

- lightness
- storage and transportability (9 m MadFlex can be wrapped in a roll of 20 cm)
- insulating capacity
- environmental impact
- possibility to avoid complex and expensive mechanisms to create folding parts
- a wide range of aesthetic finishes (also translucent)
- partial elasticity, which allows reducing vibrations, making it excellent from an anti-seismic point of view.

	Tensile Strength	**Density**	**Strength/Density Tensile ratio**	**K (thermal conductivity)**	**Light transm.**	**Elong. at break**	**Flame resistance**
	MPa	**kg/m³**		**W/(m·°C)**			
ABS	40-45*	1000-1200	0,038-0,043	0,14-0,21	-	23-30%	Low
Glass	20-200	2400-2800	0,008-0,08	0,5-1	> 80%	< 1%	Very Good
Structural Aluminium	20-520*	2640-2850	0,007-0,19	10-220	0%	3-35%	Excellent
Structural Steel	200-690*	7800-7850	0,025-0,09	17-61	0%	15-25%	Excellent
MADFLEX	40-250**	160-390**	0,12-0,6	0,04-0,06**	0-25%	3%	Very good

Table 1.2 Madflex and other material properties comparison **Yield strength **Equivalent value*

The Madflex is 5-6 times lighter than a sheet of **ABS** (polymer material) of the same flexural rigidity and 3-4 times lighter than a sheet of ABS of the same flexural resistance. Thanks to its lightness, it is more environmentally friendly: The greenhouse gases released to produce it are about half of those issued to produce an ABS panel with equivalent mechanical properties, and its insulating capacity are over 5 times higher.

Even if it is neither flexible nor insulating, today **aluminum** may be considered as one of the strongest alternatives to the MadFlex. However, in terms of stiffness and resistance, there is absolutely no comparison. In fact, a 1.8 kg 11 mm thick panel in MadFlex corresponds to a 10 kg 3.5 mm thick aluminum sheet. Moreover, from an environmental point of view, the production cost of aluminum is 5 times higher than the one of the MadFlex.

The charts show a comparison between 1mm 2mm sheets in different materials and with the same deflection under a load of 200 N.

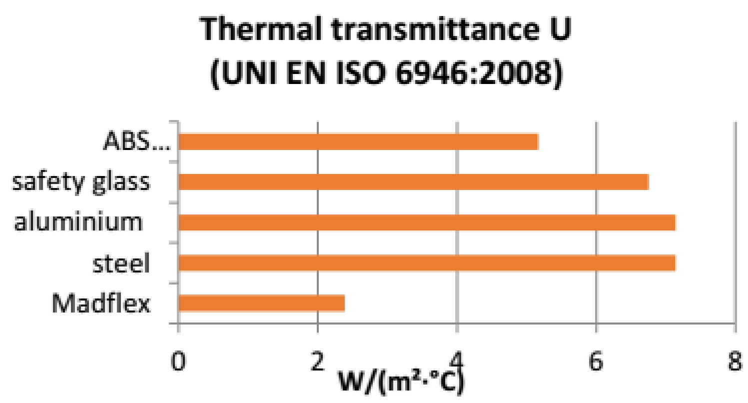

Figure 1.4 Comparative Madflex Thermal transmittance

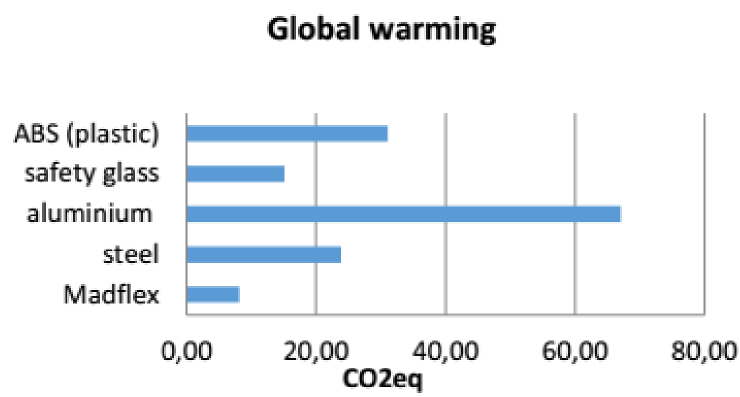

Figure 1.5 Comparative Madflex Global Warning

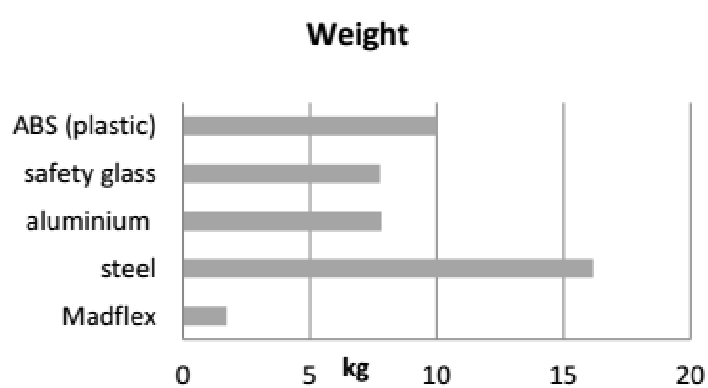

. Figure 1.6 Comparative Madflex Weight

Compared to **architectural membranes**, the Madflex is more advantageous in terms of:

• Reduction of the load on the load-bearing / supporting structures
• Reduction in weight and bulk in transport
• Insulating ability
• Increased tensile strength and stiffness, impact resistance and puncture
• Possibility to create shapes and designs otherwise impossible
• Elimination / reduction of maintenance costs and works in case of structures supported by
compressed air.

	Resistance	**Weight**	**U (thermal transm.)**	**Light transm.**	**Elong. at break**	**Flame resistance**
	kN/m	**g/m²**	**W/(m²°C)**			
VC coated olyester	45-200	520-1550	4,5 - 7,14	0-25%	18-30%	Good
FE coated berglass	124÷100	800-1500	4,5 - 7,14	10-20%	3-12%	Excellent
icone coated berglass	80÷200	605-1560	PTFE f. Similar to glass	40-50%	3-12%	Excellent
NARA® Fabric	80	1080		19-38%	10-40%	Excellent
FE film	3÷5	100-220	5,6 (1 layer) 2,9 (2 layers)	90%	300-400%	Very Good
MADFLEX	180÷600	700-1300	2,4 (1 cm) - 3,6 (0,5 cm)	0-25%	3%	Very good

Table 1.3 Madflex and other material properties comparison

The Madflex can be pasted to other materials or components during both the production phase and the following stages. Metallic parts and threaded components can be easily integrated inside or on the surface of the MadFlex. The MadFlex can be easily produced along with traditional sandwich panels, obtaining components that are rigid in some areas and flexible in others. Similarly, it is possible to create fabrics with reinforced areas in Madflex.

1.5 Aerodynamic Elements by Madflex

The combination of flexibility and stiffness of the MadFlex, coupled with its lightness, enable the development of aerodynamic elements capable of adapting their shape to different conditions, with possible applications not only in the field of sport racing, but in the entire automotive sector. Consider, for example, that a lorry traveling at 100 km / h consumes more than 60% of its fuel due to air leakage losses. The MadFlex is an ideal material for creating systems that can reduce such losses, with consequent economic and environmental benefits. For example, it is possible to create deflectors capable of connecting the cab and the trailer of a truck, reducing the air vents usually generated in this area. Other aerodynamic elements can be placed in the rear area and alongside the truck, under the trailer. One of the most problematic issue of current systems that the MadFlex can solve is given by the rigidity of the elements used, which generally interfere with the maneuvers, the maintenance operations and the opening / closing of the rear hatch.

1.6 Face Materials

Almost any structural material which is available in the form of thin sheet may be used to form the faces of a sandwich panel and also the same for the Madflex, gives a good view of the variety available in materials selection. The combination of Madflex faces has opportunity through efficient design. The properties of primary interest for the faces are;

- High stiffness giving high flexural rigidity
- High tensile and compressive strength
- Impact resistance
- Surface finish
- Environmental resistance (chemical, UV, heat, etc.)
- Wear resistance

1.7 Rigid Skin Material Properties

In the samples that are modeled in this research, the rigid face selected of a kind of Carbon fiber in which the properties are in the following,

- density: 1500 kg/m3
- carbon fiber volume: 50%
- thickness for every ply: 0.12 mm
- total thickness of a 0/90 laminate: 0.24 mm
- Elastic Modulus along fiber direction: 77.1 Gpa
- Elastic Modulus transversal direction: 2.9 GPa
- Shear Modulus 5,5 GPa
- Poisson's Ratio: 0.3

1.8 Flexible Skin Material Properties

In the Flexible face which is resistant to traction is used the Dyneema material, Ultra-high-molecular-weight polyethylene (UHMWPE) is a subset of the thermoplastic polyethylene and the properties are in the following,

- density: 1000 kg/m3
- thickness for every ply: 0.12 mm
- total thickness of a 0/90 laminate: 0.24 mm
- Tensile Modulus along fiber direction: 22 Gpa
- Compression Modulus along fiber direction: 0.5 GPa
- Elastic Modulus transversal direction: 0.1 GPa
- Shear Modulus 0.2 GPa
- Poisson's Ratio: 0.05

1.9 Core Material Properties

A kind of foam is used in the core with the following properties,

- density: 130 kg/m3
- Elastic Modulus: 60 MPa
- Shear Modulus: 30 MPa
- Thickness: 5 mm

The Geometry of the core is not continuously and its specific geometry with grooves inside that can make the new unique properties of Madflex in which in the final sandwich plane that let the sandwich stay totally rigid in bending test through in one direction and in contrary direction makes it flexible, the scheme of the core is shown in the figure 1.7

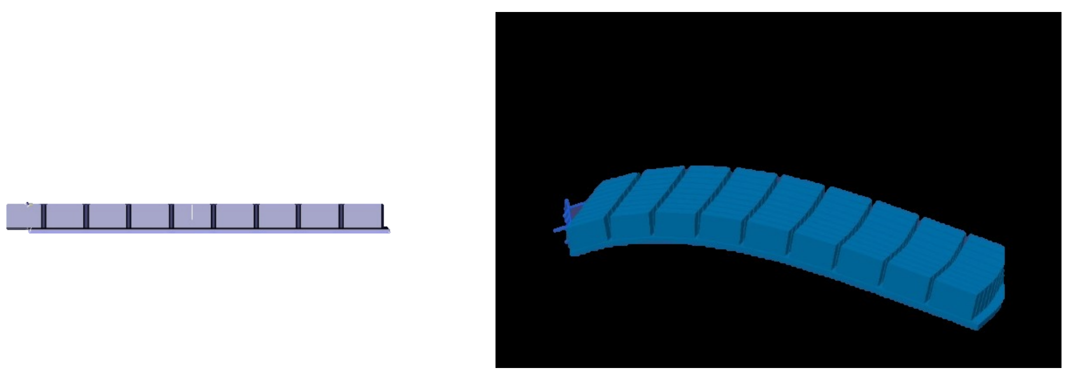

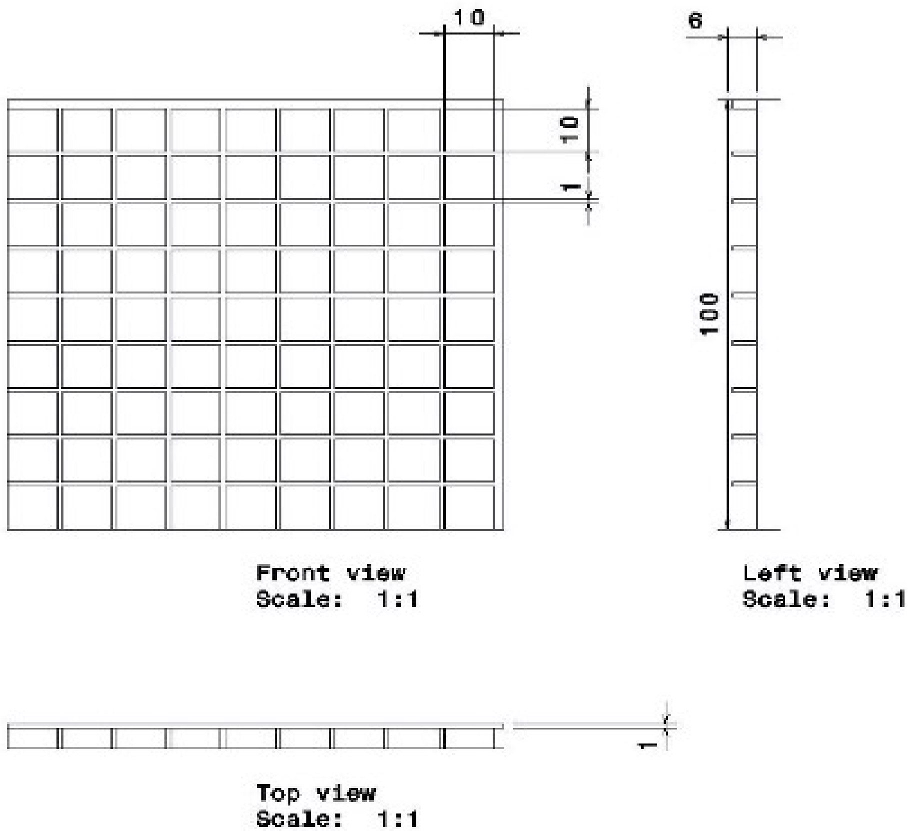

Figure 1.7 Scheme of the Madflex core

2. Introduction to Sandwich Beam Theory

2.1 BEAM ANALYSIS

In this chapter, we are going to find formula and relations for the analysis and design of convectional sandwich beams. All derivations are omitted and only the final result is presented, its limitations, if it is exact or approximate, its accuracy and how to use the formula. The theory is in much the same as ordinary engineering beam theory with the addition of shear stresses and transverse shear deformations. This theory is often referred to as the Timoshenko beam theory. For simplicity reasons, all beams are assumed to have unit width, and thus, all loads, bending moments, stiffnesses etc., are also given per unit width. The theory given here is only a summary of what is thoroughly described in the books by Allen [1] and Plantema [2]

2.2 Definitions and Sign Convention

The sign conventions used in this chapter are as illustrated in Figure 2.1 Forces and stresses are positive when in the direction of a positive coordinate when acting on a surface with a positive normal vector, e.g., σx is positive when acting on the right surface in Fig….. and in the direction of positive x-coordinate. Bending moments are positive when creating a positive deformation.

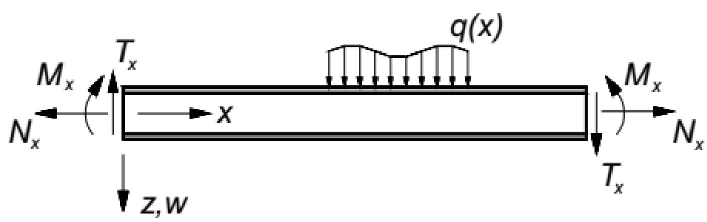

Figure 2.1 Sign convention used for stresses, force and bending moments

2.3 Flexural Rigidity

2.3.1 Symmetrical sandwich

For a symmetrical sandwich cross-section, that is when the faces are of the same material and of

equal thickness as in Figure 2.2. So, we can see

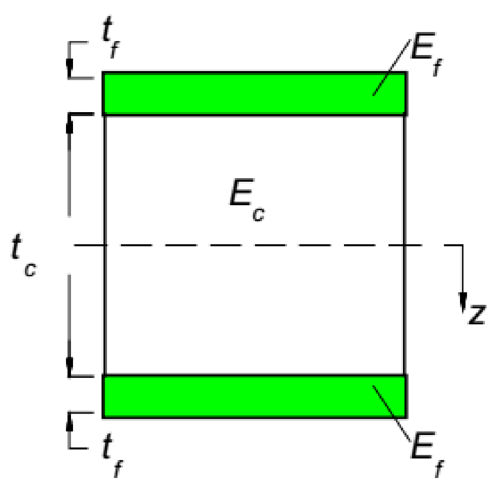

Figure 2.2 A symmetrical sandwich cross-section

$$D = \int \ E\, z^2 dz = \frac{E_f t_f^3}{6} + 2E_f t_f [\frac{d}{2}]^2 + \frac{E_c t_c^3}{12} = \frac{E_f t_f^3}{6} + \frac{E_f t_f d^2}{2} + \frac{E_c t_c^3}{12}$$
$$= 2D_f + D_o + D_c \qquad (2.1)$$

Where:

2Df is the bending stiffness of the faces about their individual neutral axes
*D*0 the bending stiffness of the faces about the middle axis
Dc the bending stiffness of the core
d the distance between the centroids of the faces, i.e., *d* = *tf* + *tc*

Thin face approximation:

$$\frac{2D_f}{D_0} < 0.01 \text{ if } 3\ (\frac{d}{t_f})^2 > 100 \text{ or } \frac{d}{t_f} > 5.77 \qquad (2.2)$$

Weak core approximation:

$$\frac{D_c}{D_0} < 0.01 \text{ if } \frac{6E_f t_f d^2}{E_c t_c^3} > 100 \qquad (2.3)$$

If *both* the above relations are satisfied, then we can approximately write

$$D = D_0 = \frac{E_f f_f d^2}{2} \qquad (2.4)$$

2.3.2 Non-symmetrical sandwich (Dissimilar faces)

A non-symmetrical sandwich cross-section is one that has dissimilar faces, that is, of different materials and/or of different thickness as in Figure 2.3

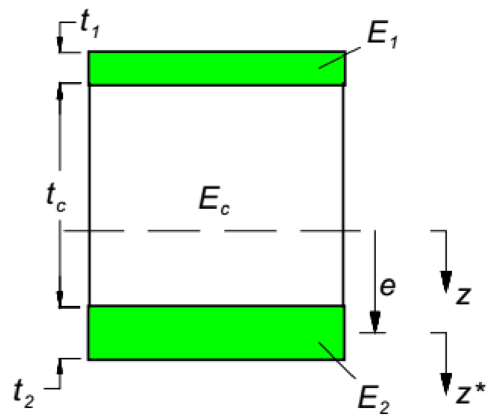

Figure 2.3 A sandwich cross-section with dissimilar faces

Before one can calculate the flexural rigidity of this cross-section, the position of the neutral axis must be found. It is given by the coordinate system for which the first moment of area is zero when integrated over the entire cross-section. The distance *e* from the middle axis of the lower face to the neutral axis is then calculated from

$$E_1 t_1 (\tfrac{t_1}{2} + t_c + \tfrac{t_2}{2}) + E_c t_c (\tfrac{t_c}{2} + \tfrac{t_2}{2}) = e[E_I t_1 + E_c t_c + E_2 t_2] \qquad (2.5)$$

The flexural rigidity is then

$$D = \frac{E_1 t_1^3}{12} + \frac{E_2 t_2^3}{12} + \frac{E_c t_c^3}{12} + E_1 t_1 (d - e)^2 + E_2 t_2 e^2 + E_c t_c (\tfrac{t_c + t_2}{2} - e)^2 \qquad (2.6)$$

where $d = t1/2 + tc + t2/2$ (distance between center lines of the faces). The sum of the two first terms may be denoted $2Df$, the sum of the third and sixth term Dc and the fourth and fifth $D0$. If the core is weak, $Ec \ll Ef$, the bending stiffness appears as (*weak core approximation*)

$$D = \frac{E_1 t_1^3}{12} + \frac{E_2 t_2^3}{12} + \frac{E_1 t_1 E_2 t_2 d^2}{E_1 t_1 + E_2 t_2} \tag{2.7}$$

and if the *both* the core is weak, $Ec \ll Ef$, and the faces are thin, $t1$, $t2 \ll tc$ (*thin face approximation*),
then

$$D = D_0 = \frac{E_1 t_1 E_2 t_2 d^2}{E_1 t_1 + E_2 t_2} \tag{2.8}$$

2.4 Stresses and Strains

2.4.1 Direct stresses and strains

The direct stresses in the faces and core due to bending equal

$$\varepsilon_X = \frac{M_x z}{D}, \text{ and thus } \sigma_f = \frac{M_x z E_f}{D} \tag{2.9}$$

thus, giving tensile stress in one face and compressive stress in the other. The coordinate z is defined as in Figure 2.3and must be measured within the face and the face modulus should that of the face considered.

$$\varepsilon_c = \frac{M_x z}{D}, \text{ and thus } \sigma_c = \frac{M_x z E_c}{D} \tag{2.10}$$

where z must be measured within the core. Hence, the direct stress varies linearly within each material constituent, but there is a jump in the stress at the face/core interface. By assuming the faces to be thin ($t1$ and $t2 \ll tc$) and the core to be weak ($Ec \ll Ef$) we can instead write

$$\sigma_{f^1} = -\frac{M_X(d-e)E_f}{D_0} \approx \pm\frac{M_X}{t_1 d} \text{ and } \sigma_{f^2} = -\frac{M_X e E_f}{D_0} \approx \pm\frac{Mx}{t_2 d} \quad (2.11)$$

with positive stress in lower face and negative in the upper, if the bending moment is positive. The direct stress and strain due to an in-plane load is simply

$$\varepsilon_{x0} = \frac{N_X}{E_1 t_1 + E_2 t_2 + E_c t_c}, \text{ and thus } \sigma_{f1} = \varepsilon_{x0} E_1, \sigma_{f2} = \varepsilon_{x0} E_2, \text{ and } \sigma_c = \varepsilon_{x0} E_c \quad (2.12)$$

where ε*x*0 is the strain in the neutral axis. The strains and stresses due to bending and in-plane loads can then be superimposed.

2.4.2 Approximations

The conclusion of the above formulae summarizes the modus operandi or the principal load carrying and stress distributions in a structural sandwich construction to; The faces carry bending moments as tensile and compressive stresses and the core carry transverse forces as shear stresses. The stress distributions for the different degrees of approximation can also be graphically represented by plotting the above equations as function *z*. By taking a symmetrical sandwich we get the relation plotted in Figure 2.4

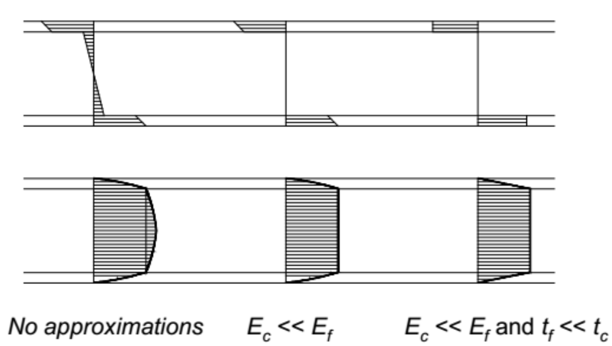

Figure 2.4 Direct and shear stresses for different levels of approximations

2.5 Deflection of a Simply-supported Sandwich Beam with Antiplane Core and Thin Faces (Symmetrical Load)

The stresses and deflections in a beam of this kind may be found, to a first approximation, by the use of the ordinary theory of bending. The theory is based on the assumption that cross-sections which are plane and perpendicular to the longitudinal axis of the unloaded beam remain so when bending takes place. This assumption leads to the well-known relationship between bending moment (M) and curvature (1 */R):*

$$\frac{M}{EI} = -\frac{1}{R} \qquad (2.13)$$

Because the faces are thin, the situation of thin faces are satisfied, the local bending stiffness of the faces is small and the first term on the right-hand side of equation (2.14) can be neglected. Also according to the situation the third term on the right-hand side of equation bellow is negligible; also, the shear stress is constant throughout the depth of the core at any given section.

$$D = E_f\frac{bt^3}{6} + E_f\frac{btd^3}{2} + E_c\frac{bc^3}{12} \qquad (2.14)$$

In the first instance the transverse displacements of the beam (w_1) may be calculated by the ordinary theory of bending, using the relationships. For example, Fig. ……..2.5b shows the bending deformation of a simply supported beam with a central point load *W.* The points *a, b, c, ...* lie on the center-lines of the faces and the cross-sections *aa, bb, cc9...* rotate but nevertheless remain perpendicular to the longitudinal axis of the deflected beam. It is obvious that the upper face is compressed as the points *a, b,* c, move closer together, while the lower face is placed in tension.

The shear stress in the core at any section is $\tau = \frac{Q}{bd}$. This is associated with a shear strain $\gamma = \frac{Q}{Gbd}$ which, like τ, is constant through the depth of the core, G is the modulus of rigidity of the core material. These shear strains lead to a new kind of deformation illustrated in Figure 2.5c. The points *a,b,c,* which lie on the centre-lines of the faces, do not move horizontally but are displaced vertically by an amount w_2. The faces and the longitudinal centre-line of the beam tilt, however, and the relationship between the slope of the beam, $\frac{dw_2}{dx}$ and the core shear strain γ may be obtained from Figure 2.6. In this diagram,

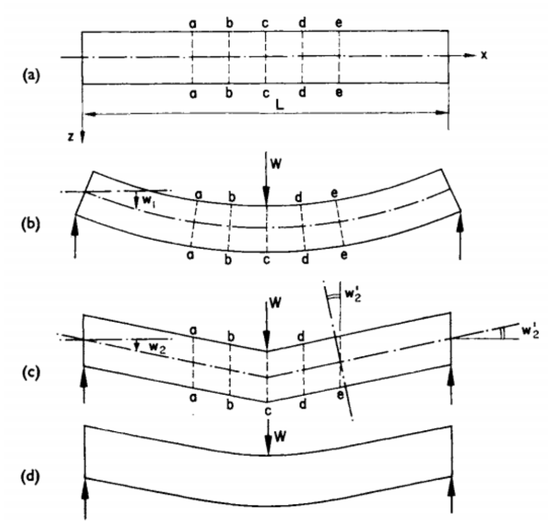

Figure 2.5 Deflection of sandwich beam

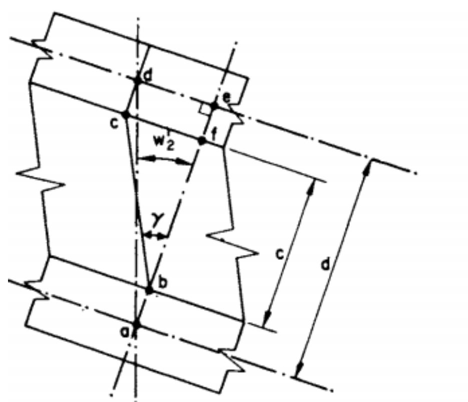

Figure 2.6 Deflection of sandwich beam

Hence,

$$\frac{dw_2}{dx} = \gamma \frac{c}{d} = \frac{Q}{Gbd} \cdot \frac{c}{d} = \frac{Q}{AG} \qquad (2.15)$$

$$A = \frac{bd^2}{c} \qquad (2.16)$$

The product *AG* is often referred to as the shear stiffness of the sandwich. The displacement w_2, associated with shear deformation of the core.

The total central deflection *Δ* is therefore the ordinary bending displacement *Δ1* with the displacement *Δ2* superimposed:

$$\Delta = \Delta_1 + \Delta_2 = \frac{WL^3}{48D} + \frac{WL}{4AG} \qquad (2.17)$$

In general, the displacement of any statically-determinate symmetrically-loaded sandwich beam with an antiplane core and thin faces may be found by similarly superimposing the bending and shear deflections w_1 and w_2.

2.6 General Buckling

2.6.1 Buckling of column - thin faces

In the buckling analysis of sandwich columns, transverse shear deformations must be accounted for. This decreases the buckling load compared with the ordinary Euler buckling cases. The critical buckling load can approximately be written as

$$\frac{1}{P_{cr}} = \frac{1}{P_b} + \frac{1}{p_s} \qquad (2.18)$$

where P_b is the buckling load in pure bending and P_s in pure shear. These are given by

$$P_b = \frac{n^2 \pi^2 D}{(\beta L)^2} \text{ and } P_s = S \qquad (2.19)$$

where the factor β depends on the boundary conditions as given in Figure 2.7 The buckling load can also be written

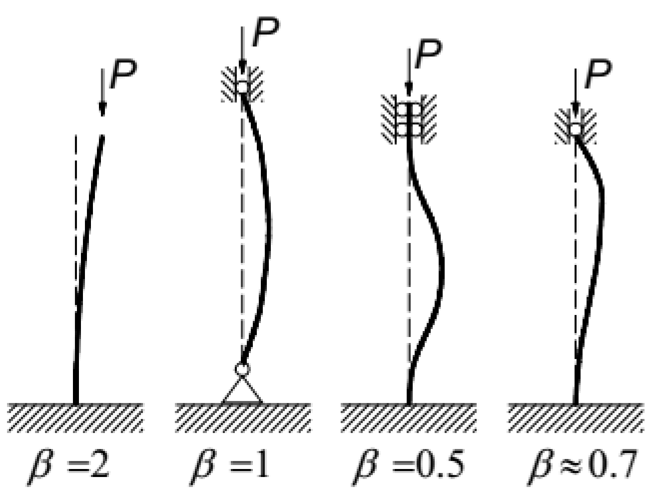

Figure 2.7 Euler’s buckling cases

$$P = \frac{n^2\pi^2 D/(\beta L)^2}{1 + n^2\pi^2 D/S(\beta L)^2} \tag{2.20}$$

Thus, when the column is long and/or has infinite shear stiffness (pure bending)

$$\lim_{S\to\infty \text{ and/or } L\to\infty} P_{cr} = \frac{n^2\pi^2 D}{L^2} = P_b \tag{2.21}$$

If, on the other hand, the beam is very short and/or is weak in shear the limit will be

$$\lim_{S\to 0 \text{ and/or } L\to 0} P_{cr} = S = P_S \tag{2.22}$$

2.6.2 Buckling of column - thick faces

When accounting for the thickness of the faces the above formula takes a slightly different form since it must be derived from another governing equation. The result can be written

$$P = \frac{\dfrac{2n^4\pi^4 D_f D_0}{S(\beta L)^4} + \dfrac{n^2\pi^2 D_0}{(\beta L)^2}}{1 + \dfrac{n^2\pi^2 D_0}{S(\beta L)^2}} \tag{2.23}$$

In this case there is another limit when the column is very short or weak in shear, namely

$$\lim_{S\to 0 \text{ and/or } L\to 0} P_{cr} = \frac{2\pi^2 D_f}{(\beta L)^2} \tag{2.24}$$

that is, the buckling load approaches infinity even for short and/or shear weak columns.

2.6.3 Buckling stress exceeding elastic limit

If the stress in the faces computed using the above formulae exceeds the limit of proportionality, yield stress or an offset strength, the elastic modulus of the faces must be replaced by a reduced modulus in order to yield an accurate buckling load. Thus, if $\sigma_f > \sigma_y$ then E_f should be substituted with E_r according to

$$E_r = \frac{2E_f E_{tan}}{E_f + E_{tan}} \tag{2.25}$$

where E_{tan} is the tangent modulus at the given point on the stress-strain relation according to Figure 2.8 and σ_y the yield strength.

In the strain regime considered most core materials can be assumed linear elastic. The internal load of the column hence equals

$$P = 2t_f\sigma_f + t_c E_c \varepsilon_f \tag{2.26}$$

Since the buckling load is a function of E*tan* is it also a function of εf Thus, at some point on the stress-strain curve the internal load, as given above, equals the buckling as calculated in (*2.25*) or (*2.26*) above but with *E* substituted for *Er*. The instability load is then found as the point on the stress-strain curve where the buckling load equals the internal load *P*.

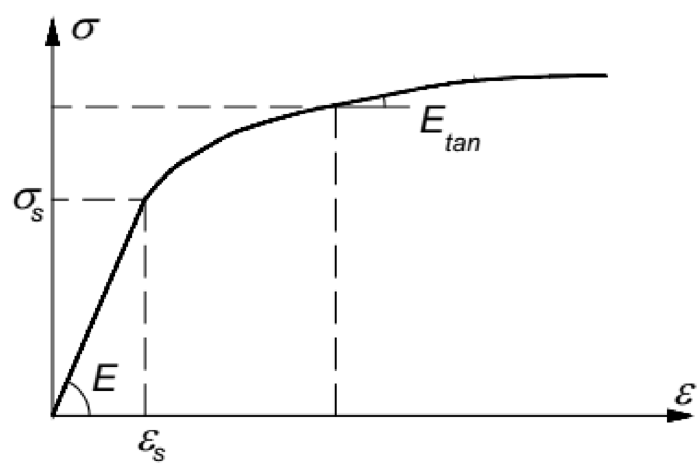

Figure 2.8 Schematic of stress-strain relation for the face material

2.7 Local Buckling of Sandwich Beams

Local buckling is a form of local instability of the face sheet. It can be seen as buckling of a thin strip of material (the face) supported by a continuous or discontinuous elastic medium, the core. Schematically it looks like in Figure 2.9

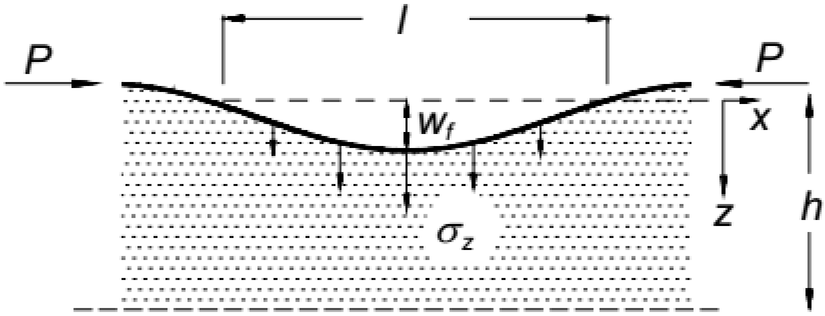

Figure 2.9 Schematic of local face buckling

This kind of instability can occur whenever a face sheet is in compression, that is, not only when the in-plane load resultant is negative but also in pure bending since then one face exhibits membrane tension and the other membrane compression.

The face is assumed to deform as

$$w_f = W \sin\frac{\pi x}{L} \tag{2.27}$$

where L is wavelength of the buckle which can be estimated by

$$L = \pi\left(\frac{4D_f^2}{E_c G_c}\right)^{1/6} \tag{2.28}$$

The actual instability load can be derived in several ways. The mode of buckling changes from symmetrical to unsymmetrical depending on the core thickness and the actual buckling load then depends on the ratio *tf/tc*. The exact solution to this problem has been found to yield nonconservative results mainly due the fact that initial imperfections has a quite large effect on the local buckling load. For practical purposes the following formula has shown to yield very good results.

$$\sigma_f = 0.5\sqrt[3]{E_f E_c G_c} \tag{2.29}$$

In the case of an isotropic plate, simply substitute E_f for $E_f / (1-\nu_{2f})$ and E_c for $E_c / (1-\nu_{c2})$.

3. Standard Bending Test on Madflex

3.1 Specimen

The most important stage of finding the properties of a model and specimen and design or verification a new sample also to verification of the manufacturing process is testing. In the first step, the raw material properties should be considered as the inputs of Finite Element applications. Also, we can find the properties of the material by three different methods, the first way to find the properties of the material is to find them in the book and references or other ways is to find from calculation or estimations, the other way is testing material to obtain its properties. Using handbooks is not a precise way to have a particular design because some properties of materials, particularly in composite materials is a function of ambient properties also the manufacturing process like lay-up of fibers and sequence.

Theoretical estimation maybe works as a useful tool for the first steps of designing to get approximate for the mechanical properties but in the other stages we need more accurate data then in this stage we need testing to get precise results.

Testing is sometimes vital to analyze a structure during the design process to verification physical properties. Maybe by calculation, it takes a lot of time therefore in this situation by testing the structure or even some part of that, we could have an accurate result.

this chapter describes the bending test applied on the Madflex that is the same as the test that usually applied on the conventional sandwich to have some experimental data of Madflex and then we can verify the FEM results with experimental data from the tests.

3.2 Flexural Behavior of Sandwich Composite Panels Under 4-Point Loading

3.2.1 Aim and Purpose of Test Methods

The flexural test or bending test is usually performed according to ASTM D7250/7250M standard on the sandwich structures therefore in the case of Madflex we have performed the same test that is performed on the conventional sandwich but in the case of Madflex, the behaviors of each side of that are not to same so we must do the test separately for each face and all the analysis is done differently for each side of Madflex. We are going to apply this test on the three different samples in the rigid face of Madflex to obtain the Bending stiffness of Madflex.

3.2.2 Specimen types, Dimensions and Manufacturing

The sample that we have used in this test is a Madflex with two layer of woven carbon layer in one face and two layers of woven Dyneema in the other face. The core is a foam with 5mm thickness. The geometry and dimension of the sample is shown in the Figure 3.1

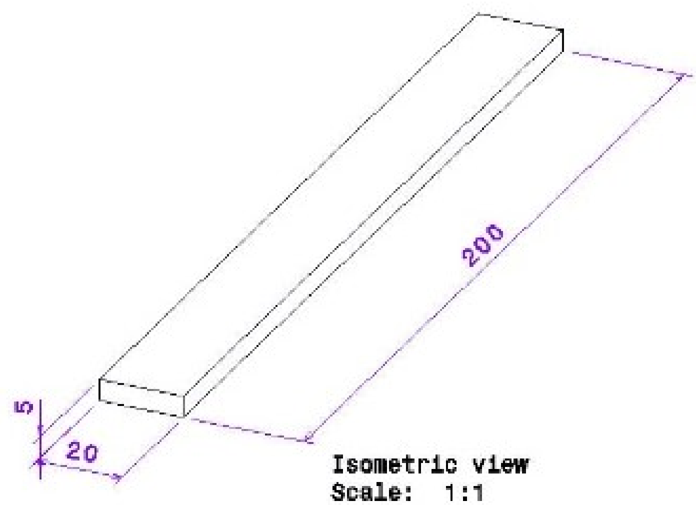

Figure 3.1 The geometry and dimension of the sample

The test is performed with two supports with 200mm distance and two rolls between them with distance of 80mm. Figure 3.2

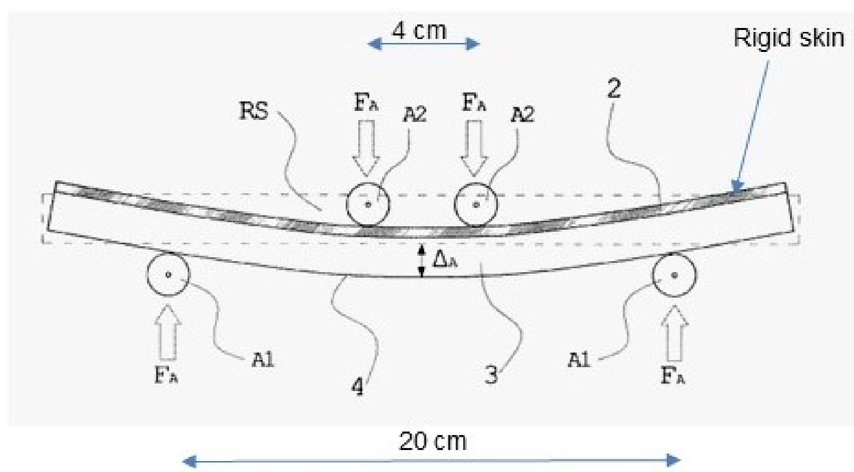

Figure 3.2 standard geometry of test

3.3 Analytical Formulation

This study calculated the mechanical properties using the simplified beam theory as proposed by ALLEN [1], Initial evaluation on the effect of gluing on the stiffness of the composite sandwich beam was conducted. The Flexural stiffness, EI of the sandwich panel is being calculated using the elastic properties of the fiber composite skins and core material and simple sandwich beam theory. For a sandwich beam, the equivalent flexural rigidity $(EI)_{eq}$ consists of the sum of the rigidities of the faces and core measured about the centroidal (neutral) axis M-M of the entire cross section as shown in the figure 3.2 The standard 4- point loading have the centerlines of the support bars separated by a distance of L= 200 mm as shown in figure 3.1 The support bars are free rotation of the specimen at the loading and support point.

[1] Allen HG. Analysis and design of structural sandwich panels. London (UK): Pergamon Press; 1969.

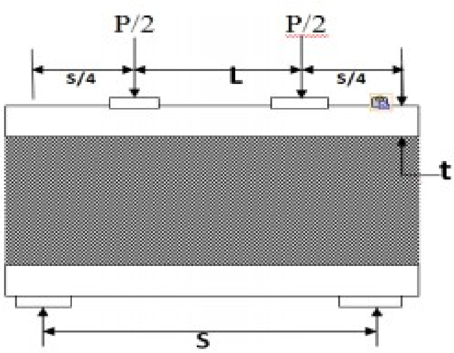

Figure 3.1 4-point loading

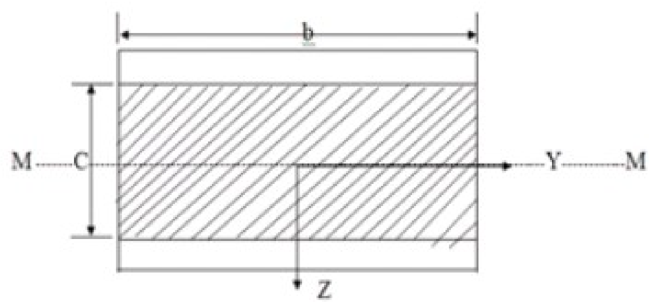

Figure 3.2 Cross section area of the specimen

$$(EI)_{core} = \frac{bc3}{12} E_C \quad (3.1)$$

$(EI)_{core}$ = Flexural Stiffness of Core Material

$(EI)_{face}$ about M-M axis = $E_f I_{face}$

I_{face} can be calculated from the parallel axis theorem.

$$I_{face} = 2\left[I_{faces} + \text{Area}\,(d/2)^2\right] \quad (3.2)$$

$$\mathbf{(EI)_{faces}} = E_f\,[bt^3/12 + btd^2/2]$$

(3.3)

The standard formulas for flexural stiffness was calculated using ASTM standards

$$\mathbf{EI} = \left[\frac{bt^3}{6} + \frac{btd^2}{2}\right] E_S + \frac{bC^3}{12} E_C$$

(3.4)

Where:
EI = Flexural Stiffness
b = width of the specimen
t = Skin thickness
c = Core thickness
d = Specimen thickness
E_S, E_C = Skin and core Young's Modulus

The deflection of the beam was then calculated using ASTM D 7250/D 7250M-06 standard.

$$\delta = \frac{P\,(2S^2 - 3SL^2 + L^3)}{96EI} + \frac{P\,(S - L)}{4U}$$

(3.5)

Where:
P = Load applied on the specimen (N)
L = Load span Length (mm)
U = Transverse shear rigidity (Mpa)
S = Support span length (mm)

3.4 Results

3.4.1 Rigid Side

According to the previous information, the behavior of Madflex in the opposite direction of bending is totally different, therefore we are going to perform two different tests for each side. In the following, some output of the bending test is shown in the table 3.1

Time [ms]	Deformation [mm]	Force [kg]		Force [N]	Mmax (N*m/m)	Deformation [mm]
16	0	0.54		5.2974	10.5948	0
31	0	0.55		5.3955	10.791	0
47	0	0.55		5.3955	10.791	0
64	0	0.54		5.2974	10.5948	0
81	0	0.54		5.2974	10.5948	0
99	0	0.56		5.4936	10.9872	0
116	-0.00333	0.56		5.4936	10.9872	0.00333
131	-0.00333	0.55		5.3955	10.791	0.00333
148	-0.00333	0.55		5.3955	10.791	0.00333
165	-0.00666	0.55		5.3955	10.791	0.006664
182	-0.00666	0.55		5.3955	10.791	0.006664
199	-0.00999	0.55		5.3955	10.791	0.009995
215	-0.01332	0.56		5.4936	10.9872	0.013325
231	-0.01332	0.56		5.4936	10.9872	0.013325
248	-0.01665	0.56		5.4936	10.9872	0.016655
265	-0.01999	0.56		5.4936	10.9872	0.019989
282	-0.02332	0.56		5.4936	10.9872	0.023319
299	-0.02665	0.56		5.4936	10.9872	0.026649
316	-0.02998	0.56		5.4936	10.9872	0.029984
332	-0.03331	0.56		5.4936	10.9872	0.033314
348	-0.03664	0.56		5.4936	10.9872	0.036644
364	-0.03998	0.56		5.4936	10.9872	0.039978
382	-0.04331	0.57		5.5917	11.1834	0.043308
399	-0.04997	0.57		5.5917	11.1834	0.049969
416	-0.0533	0.57		5.5917	11.1834	0.053303
432	-0.05663	0.58		5.6898	11.3796	0.056633
449	-0.05996	0.58		5.6898	11.3796	0.059963
465	-0.06663	0.58		5.6898	11.3796	0.066628
482	-0.06996	0.58		5.6898	11.3796	0.069958
499	-0.07662	0.58		5.6898	11.3796	0.076622
515	-0.07995	0.58		5.6898	11.3796	0.079952
532	-0.08662	0.59		5.7879	11.5758	0.086617

549	-0.08995	0.59		5.7879	11.5758	0.089947
566	-0.09661	0.59		5.7879	11.5758	0.096611
582	-0.10327	0.59		5.7879	11.5758	0.103271
598	-0.10994	0.59		5.7879	11.5758	0.109936
615	-0.11327	0.59		5.7879	11.5758	0.113266
632	-0.11993	0.59		5.7879	11.5758	0.11993
649	-0.12659	0.59		5.7879	11.5758	0.126591
666	-0.13326	0.61		5.9841	11.9682	0.133255
682	-0.13992	0.61		5.9841	11.9682	0.139919
698	-0.14658	0.61		5.9841	11.9682	0.14658
716	-0.15324	0.61		5.9841	11.9682	0.153244
732	-0.1599	0.61		5.9841	11.9682	0.159904
749	-0.16657	0.61		5.9841	11.9682	0.166569
766	-0.17323	0.61		5.9841	11.9682	0.173233
782	-0.17989	0.63		6.1803	12.3606	0.179894
798	-0.18656	0.63		6.1803	12.3606	0.186558
815	-0.19322	0.63		6.1803	12.3606	0.193218

Table 3.1 Experimental bending test results of rigid side

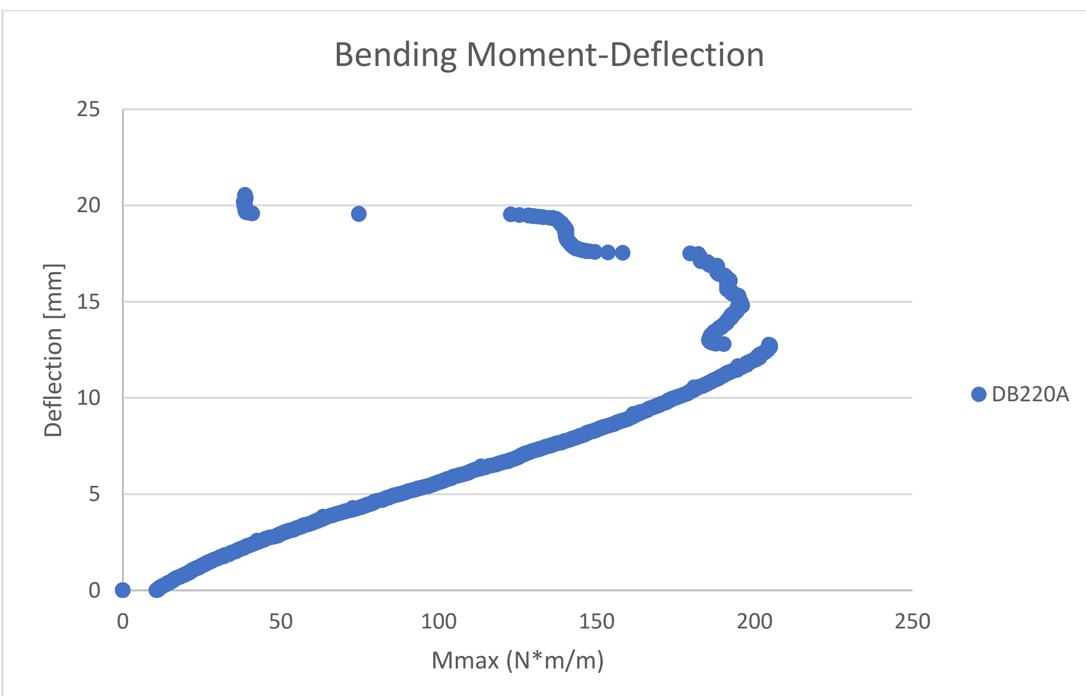

Figure 3.3 Bending Moment-Deflection of first sample

As was mentioned before the test applied on the rigid side of three similar samples as DB220A, DB220B, DB220C, and the force from 0 to 100 N applied on the samples, and then we can draw a graph of deflection as a function of bending moment.

It's illustrated in the graph Figure 3.4 the results of the three samples, and as we can see the behavior of Madflex in three samples is more or less similar.

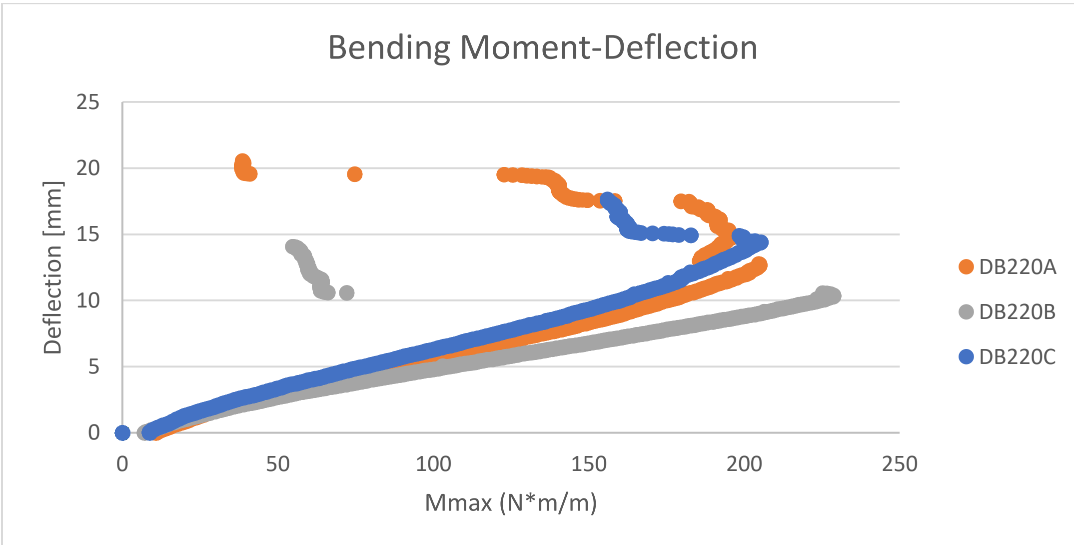

Figure 3.4 Bending Moment-Deflection of three samples

We can simply calculate the bending stiffness of the beam according to the results. Bending stiffness of a beam or rod also known as flexural rigidity. This parameter defined as EI where E is young modulus and I is second momentum of area. Bending stiffness has SI unit of $[N \cdot m^2]$.

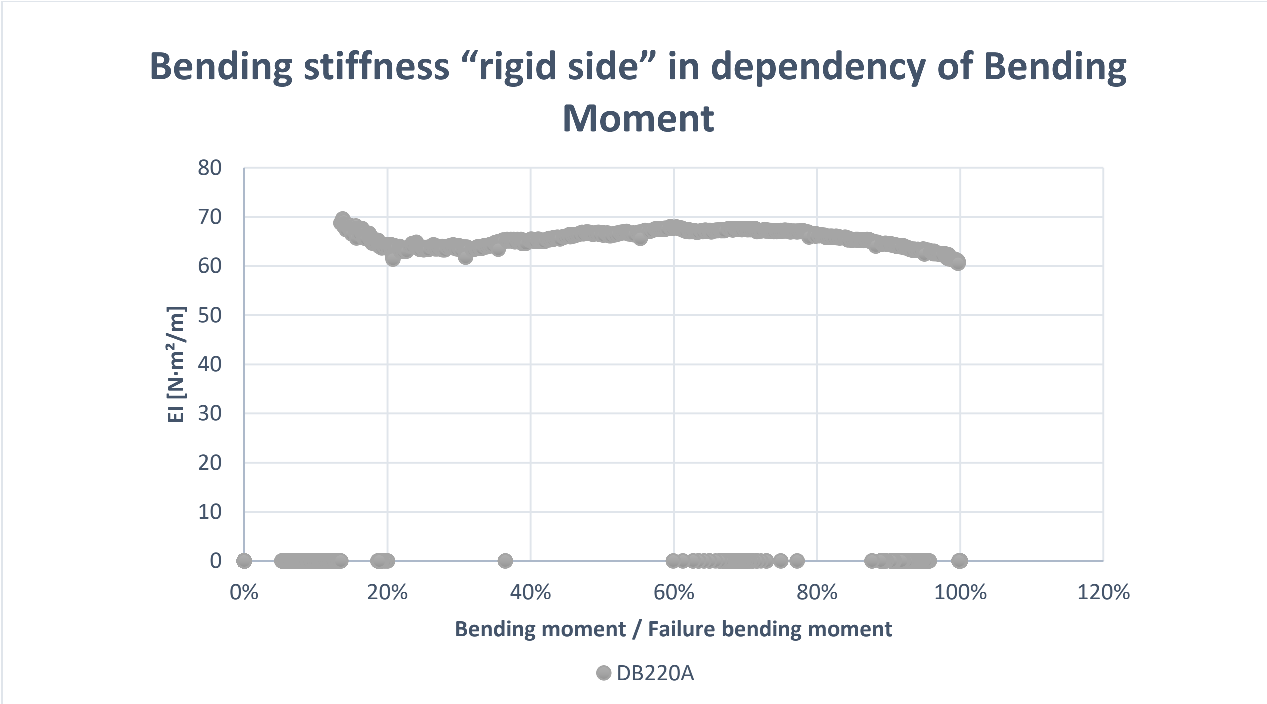

Figure 3.5 Bending stiffness of sample DB 220A

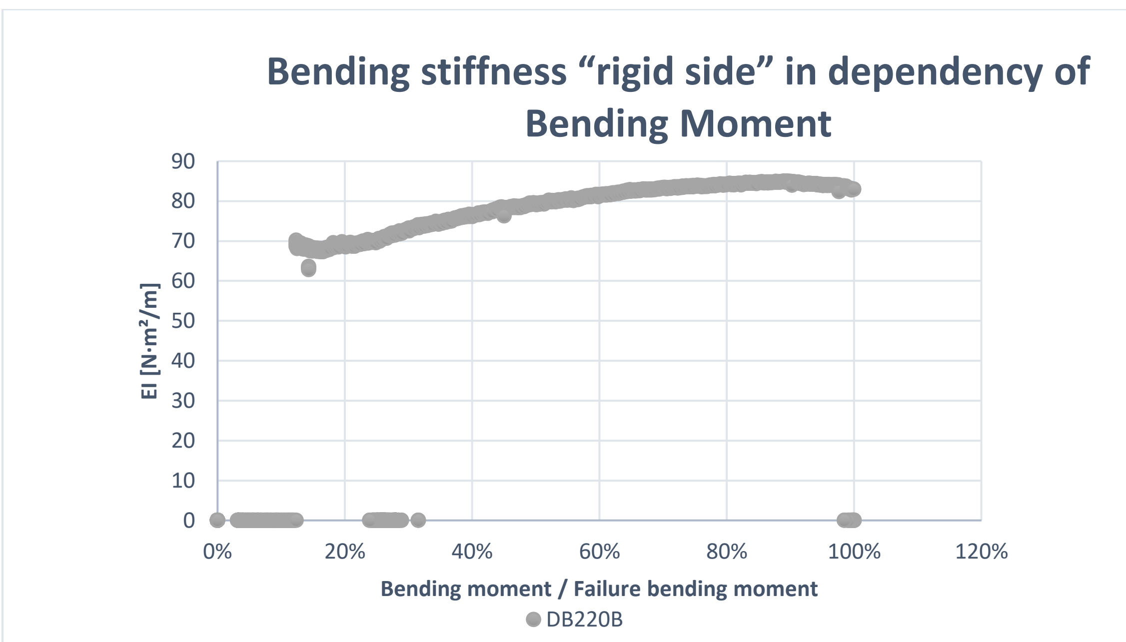

Figure 3.6 Bending stiffness of sample DB 220B

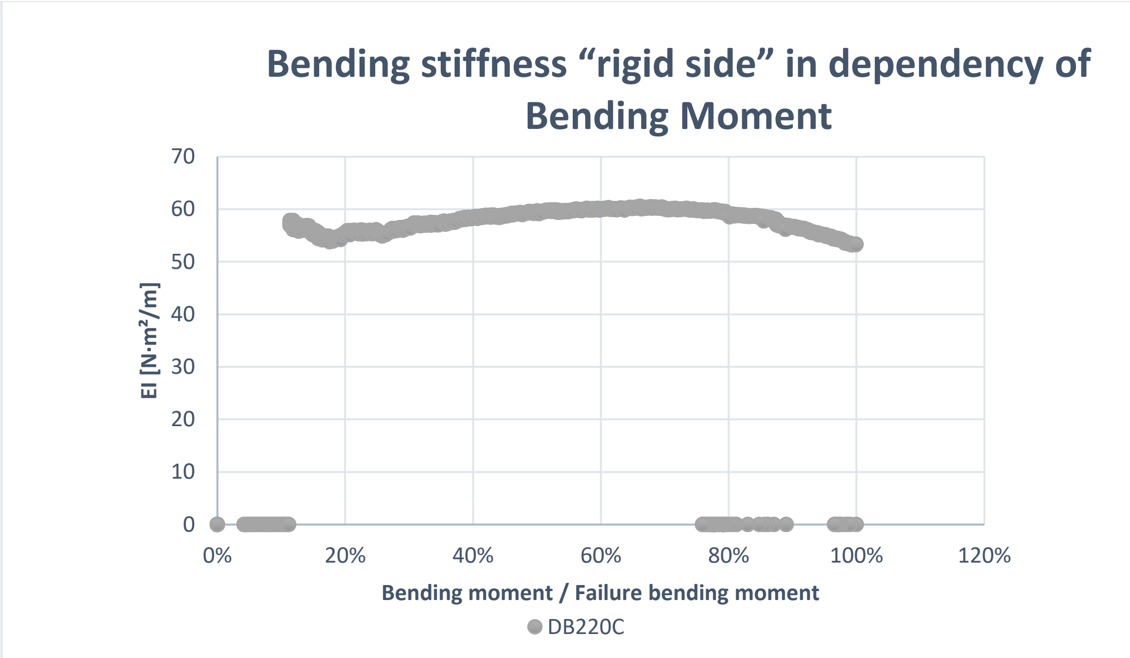

Figure 3.7 Bending stiffness of sample DB 220C

3.4.2 Flexible side

According to the previous information, the behavior of Madflex in the opposite direction of bending is totally different, therefore we are going to perform two different tests for each side. Now we have performed the test on the flexible side, some output of the bending test is shown in the table3.2

Time [ms]	Deformation [mm]	Force [kg]		Force [N]	Mmax (N*m/m)	Deformation [mm]
15	-3.50795	0.05		0	0	3.50795
32	-3.50795	0.05		0	0	3.50795
48	-3.50795	0.05		0	0	3.50795
65	-3.50795	0.05		0	0	3.50795
82	-3.50795	0.05		0	0	3.50795
99	-3.50795	0.06		0.0981	0.1962	3.50795
116	-3.50795	0.06		0.0981	0.1962	3.50795

132	-3.50795	0.05		0	0	3.50795
148	-3.50795	0.05		0	0	3.50795
164	-3.50795	0.05		0	0	3.50795
182	-3.50795	0.05		0	0	3.50795
198	-3.50795	0.05		0	0	3.50795
215	-3.50795	0.05		0	0	3.50795
231	-3.50795	0.05		0	0	3.50795
248	-3.50795	0.04		-0.0981	-0.1962	3.50795
263	-3.50795	0.04		-0.0981	-0.1962	3.50795
282	-3.50795	0.05		0	0	3.50795
299	-3.50795	0.05		0	0	3.50795
315	-3.50795	0.05		0	0	3.50795
333	-3.50795	0.05		0	0	3.50795
348	-3.50795	0.05		0	0	3.50795
365	-3.50795	0.05		0	0	3.50795
382	-3.50795	0.05		0	0	3.50795
399	-3.50795	0.05		0	0	3.50795
415	-3.50795	0.05		0	0	3.50795
431	-3.50795	0.05		0	0	3.50795
449	-3.50795	0.06		0.0981	0.1962	3.50795
465	-3.50795	0.06		0.0981	0.1962	3.50795
482	-3.50795	0.06		0.0981	0.1962	3.50795
498	-3.50795	0.06		0.0981	0.1962	3.50795
515	-3.50795	0.06		0.0981	0.1962	3.50795
531	-3.50795	0.05		0	0	3.50795
548	-3.50795	0.05		0	0	3.50795
565	-3.50795	0.05		0	0	3.50795
582	-3.50795	0.05		0	0	3.50795
613	-3.50795	0.05		0	0	3.50795
626	-3.50795	0.05		0	0	3.50795
641	-3.50795	0.05		0	0	3.50795
658	-3.50795	0.06		0.0981	0.1962	3.50795
673	-3.50795	0.06		0.0981	0.1962	3.50795
690	-3.50795	0.06		0.0981	0.1962	3.50795
705	-3.50795	0.06		0.0981	0.1962	3.50795
722	-3.50795	0.06		0.0981	0.1962	3.50795
738	-3.50795	0.05		0	0	3.50795
756	-3.50795	0.05		0	0	3.50795
773	-3.50795	0.06		0.0981	0.1962	3.50795
790	-3.50795	0.06		0.0981	0.1962	3.50795
807	-3.50795	0.05		0	0	3.50795

Table 3.2 Experimental bending test results of flexible side

Similar to rigid side of Madflex we have performed the test on the three different sample which named in the graphs as DB220AB2, DB220AB10 and DB220CB2.

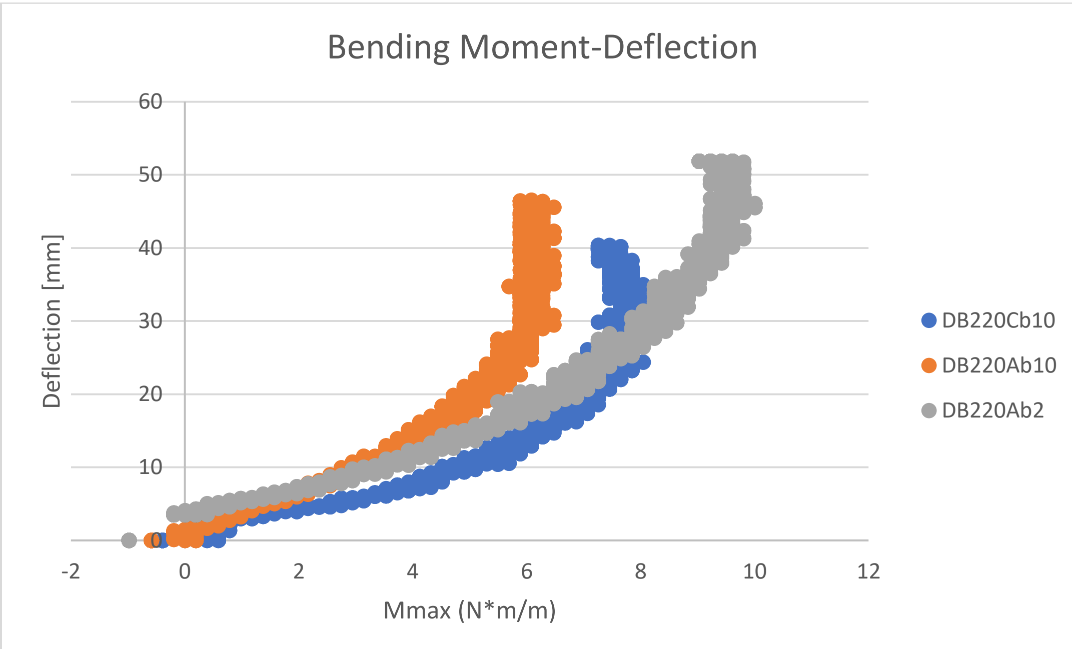

Figure 3.8 Bending Moment-Deflection of three samples flexible side

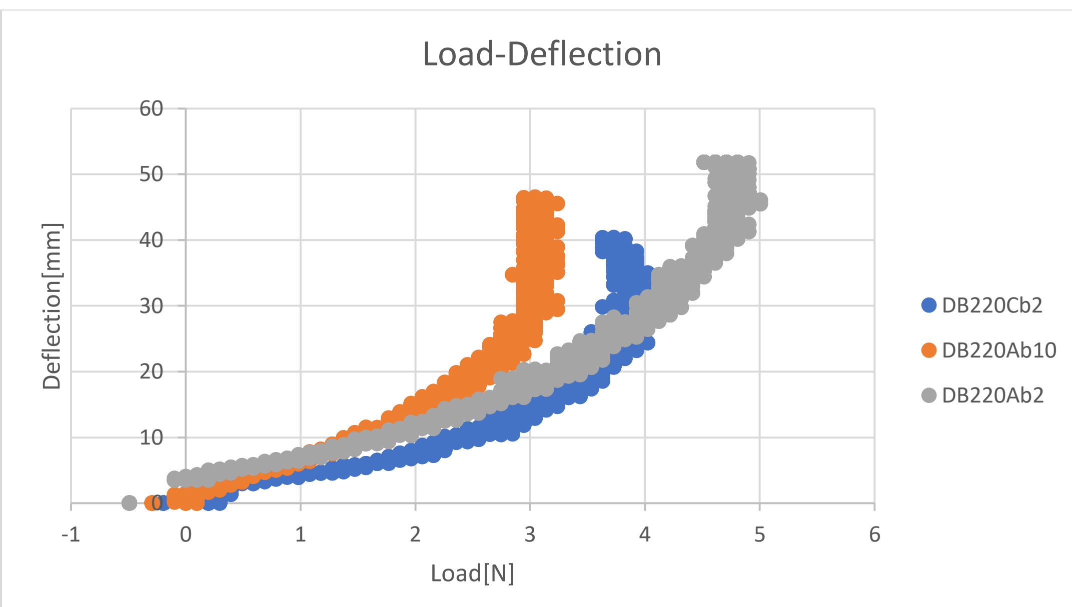

Figure 3.9 load-deflection of three samples flexible

4. FEM Results

4.1 Finite-Element Modeling

As briefly explained the focal point of the research is the investigation of a finite-element method for analysis Madflex so as a starting point we are going to simulate the experimental test in PATRAN then we can compare the maximum deflection in the NASTRAN results with the experimental test.

So, to this goal, after preparing the geometry of the core of Madflex we must start meshing that, for this purpose, we need a different kind of meshing on the model. In this modeling, we used 3D, Hex8 and for the faces, we used 2D elements Quad4 and we used the command equivalent to integrate the nodes.

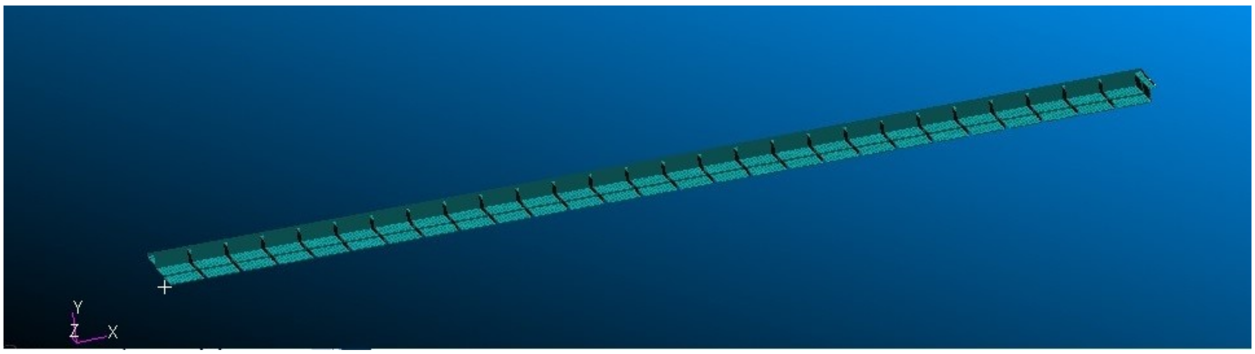

Figure 4.1 Core,3D Elements, HEX8

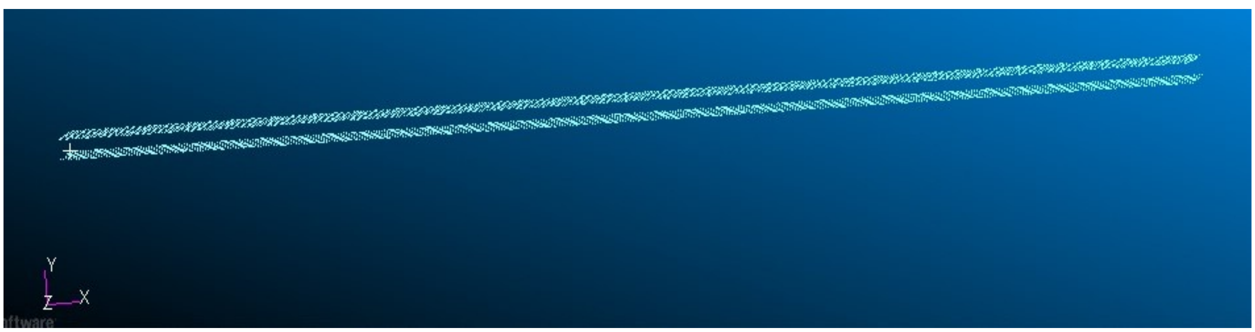

Figure 4.2 Faces,2D Elements, QUAD4

4.2 Boundary Conditions

According to the experimental standard test, it is performed with two supports with 200mm distance and two rolls between them with a distance of 80mm. The supports fix the specimen along the y-direction and also we know that there is not any forced transfer along the z-direction, therefore, zero displacements constrain along the z,y directions are applied on the two supports.

By considering the sample during the experimental test its visible that the surface of the sample can sild on the supports as the force and deflection of the beam is increasing, so it's free of constraining along the x-direction, to sum up, we have applied zero displacements along the z,y and free along the x-direction as it can be defined in Patran by < ,0,0> .

The forces applied on the sample along the y-direction so we have considered the vertical loads in the section of the sample as we can see in the Patran menu like <0,F,0>.

4.3 Solution Type

According to the Patran options, it's possible to select linear and non-linear static analysis to solve the problem in the NASTRAN.

The simulations are totally performed in the linear static form, For the rigid configuration of Madflex. and also, according to the experimental test, the local failure of Dyneema didn't happen in the flexible configuration, so we have also considered the linear static solution for the flexible part of the test.

4.4 Foam Properties change after Curing

According to the manufacturing process, the Carbon face, Dyneema face, and Foam lay-up on the molding surface. Between the faces and foam, we have used a film of resin to bond the structure together. Then the materials will be covered with a thin layer of vacuum bagging film to prepare the sample for curing.

After analyzing the final sample and the raw foam by a microscope, we observed some porosity on the surface of the foam that is filled by the resin, and by some experimental test, we find out that the resin penetrates the foam porosity by 1mm and it makes a new layer on the foam with new properties that can totally change the properties of the final Madflex.

Therefore, after the laboratory information, we conclude that we have to model a thin layer in the FEM simulation with 0.5mm Hight and 3000Mpa of elastic tension modulus.

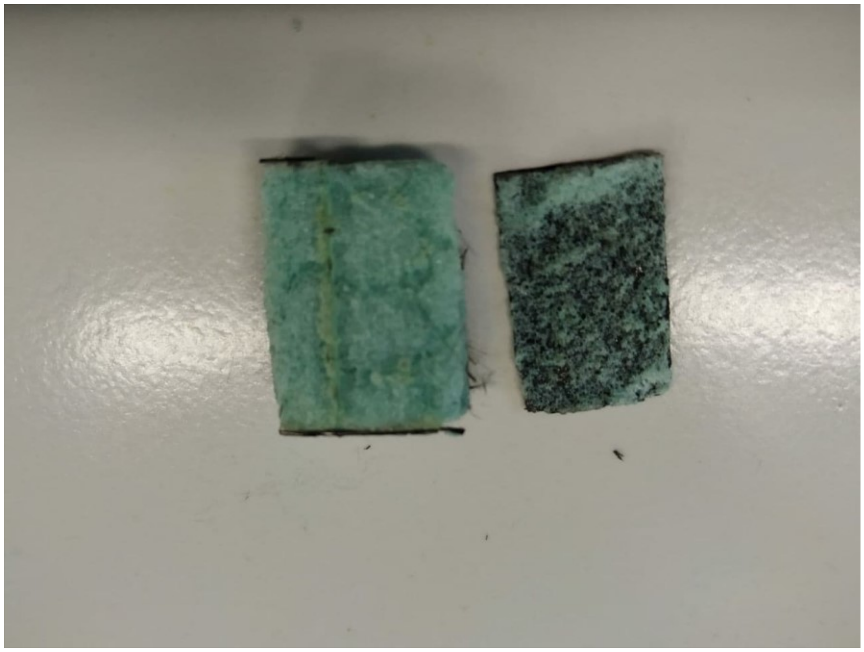

Figure 4.3 Foam Properties change after Curing

4.5 Rigid Face of Madflex

The results of the modelling plate are shown in Figure 4.4. The static analysis applied to this model and two distributed force (3.09 N) applied on the rigid face and as we can see in the picture the maximum deformation applied on nude number 29844 and the value of deformation is 0.688 mm.

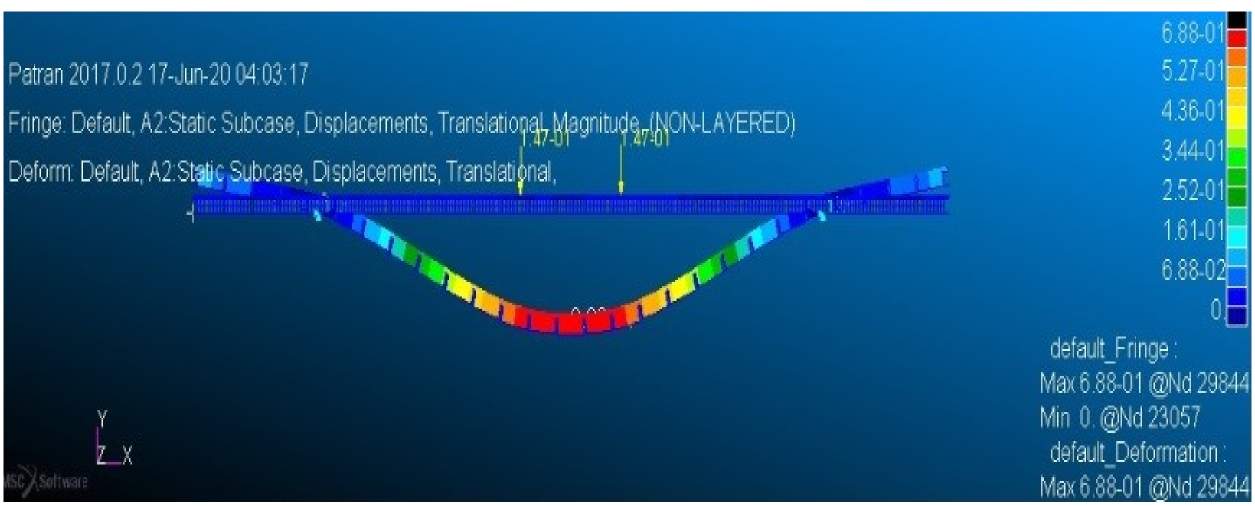

Figure 4.4 FEM result of rigid face

As was mentioned before the test applied on the rigid side of three similar samples as DB220A, DB220B, DB220C, and the force from 0 to 100 N applied on the samples, and then we can draw a graph of deflection as a function of bending moment. The curve of each sample and the FEM static analysis is drowned on the same graph in Figure 4.5

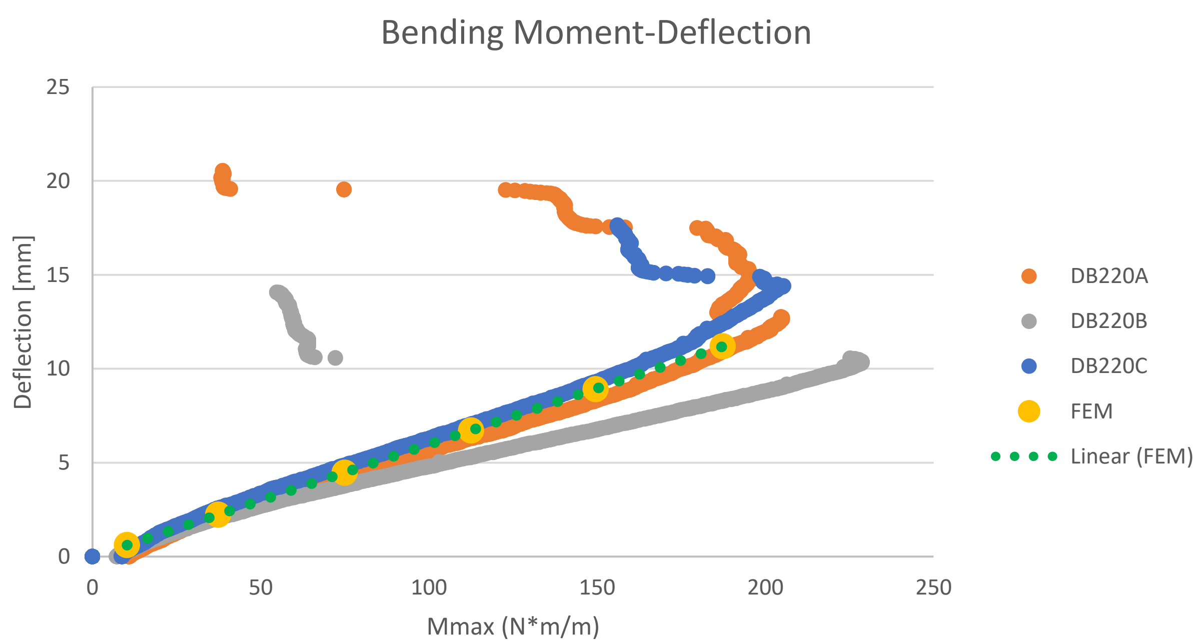

Figure4.5 FEM and experimental

4.6 Flexible Face of Madflex

It’s totally different to analyze the flexible side of Madflex. According to the core geometry of Madflex, there are some grooves in touch with Dyneema face and Dyneema face is under tension stress when the sample tends to bend on the flexible side therefore by observing the experimental sample it's clearly visible that the Dyneema face on the grooves sections is broken and these broken parts are creating due to local Buckling phenomenon.

The local Buckling phenomenon of Dyneema face leads to zero distribution of load on this face, so in the FEM analysis of Madlex to the flexible face, we can eliminate the Dyneema and perform the FEM modeling with very low properties of Dyneema. In the following figure, we can explicitly see the local Buckling in the FEM simulation. This result happens when we do Non-linear static analysis in NASTRAN.

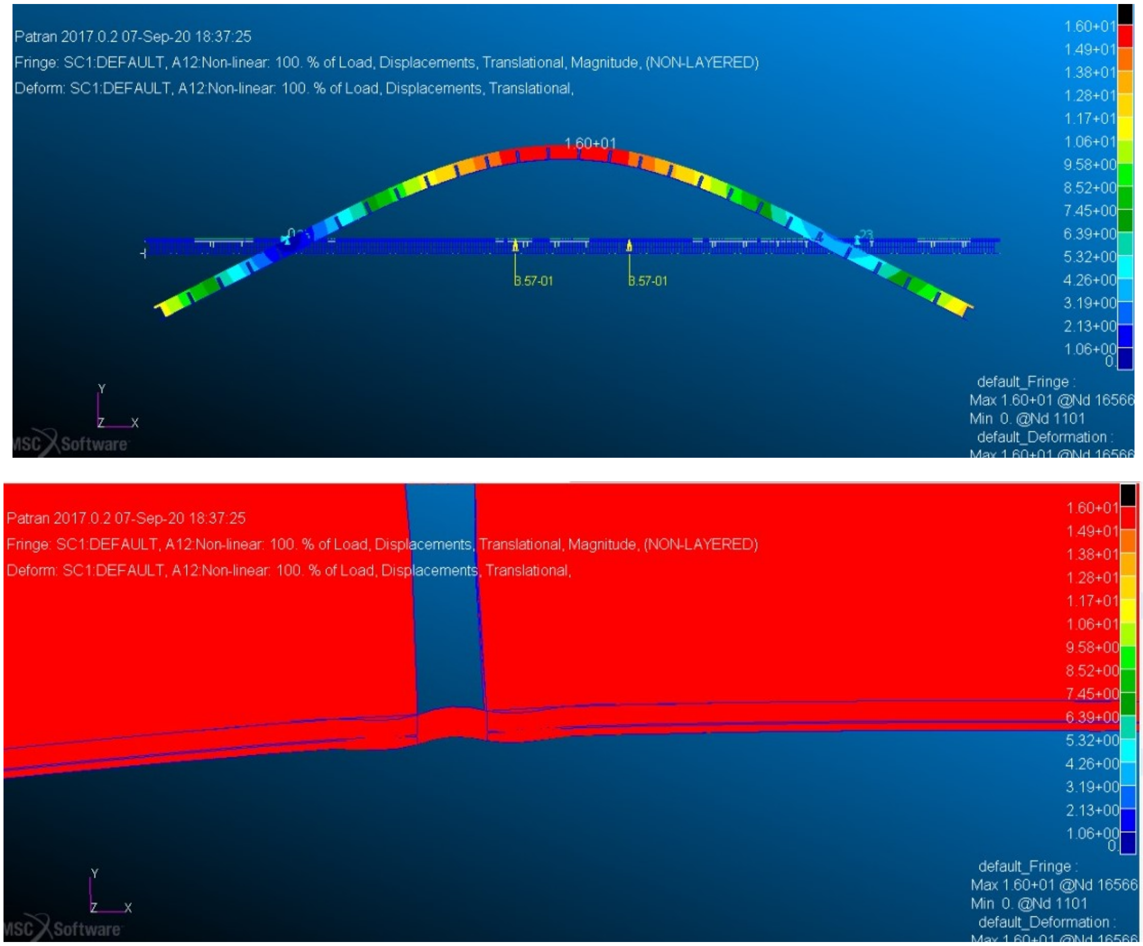

Figure 4.6 deflection of Madflex analysis by linear static solution in NASTRAN

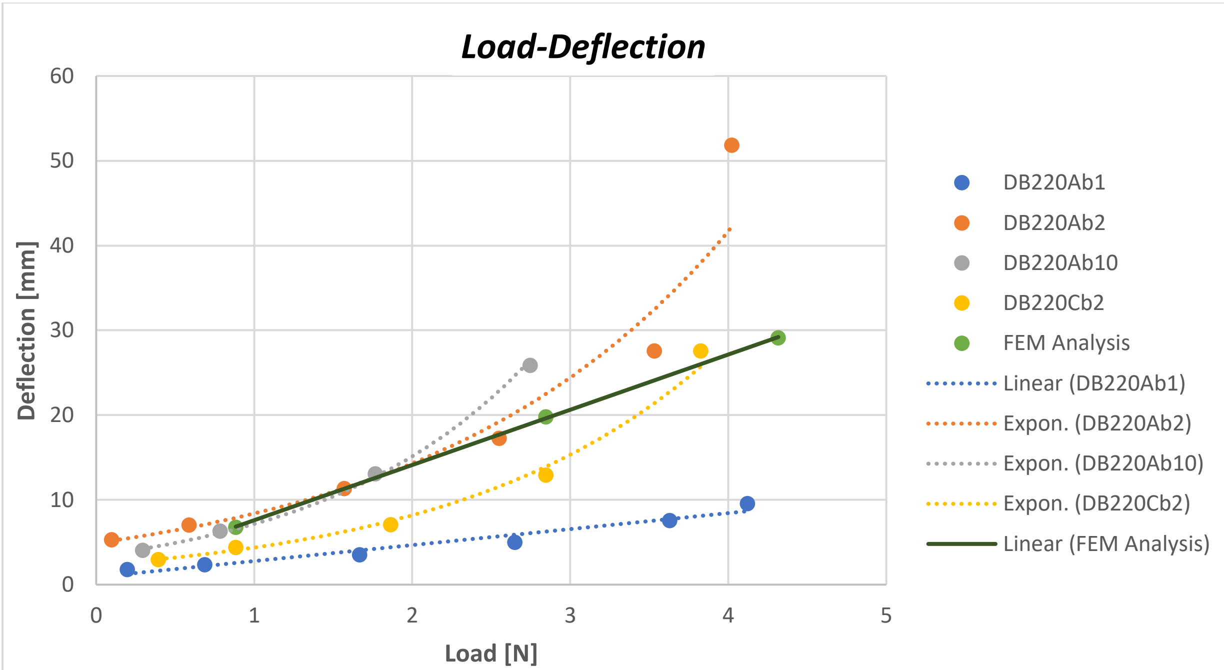

Figure 4.7 Its illustrated the load-deflection of Madflex analysis by linear static solution in NASTRAN

4.7 Conclusion

4.7.1 Interpretation of Experimental Results

According to figure 4.8 we can see the load-deflection graph of a Madflex on flexible side, as we can see in the graph, the behavior of the material is different in a different cycles of applying load.

First, we are quite sure that the carbon layer doesn't change its properties after the bending cycles. We tested some carbon laminate samples, performing the 4-points bending test for laminates, and we didn't observe relevant property variation after ten bending.

We tested also some Madflex samples also after 100000 bending cycles: we performed the 4-points bending test for the rigid side and we observed substantially the same behavior (stiffness and strength) as a virgin sample. So, the rigid skin doesn't change its compression modulus and its strength after many bending cycles. We also know that carbon fiber laminates don’t change a lot their elastic modulus for a few cycles and small tension.

Moreover, we know that carbon laminate doesn't increase its flexibility when you bend it. The experimental data of the attached graph shows that sandwich stiffness progressively decreases during the test. The only way to explain it the buckling of foam cell walls, of Dyneema layer, and of Dynema fibers.

So, we expect that the non-linearity of the experimental data depends on the progressive buckling of the UHMWPE (Dyneema) fabric layer. We know that fabric is constituted by Dyneema filaments, and the filaments are constituted by Dyneema fibers (that you can see using a magnifying glass) and the fibers are constituted by microscopic fibrils.

Unlike carbon, Dyneema fibers have exceptional flexibility in spite of the high tensile modulus, because they are constituted by fibrils which can slip and move with respect to the others; the fibrils have a diameter lower than 1 micron an order of magnitude smaller than carbon fiber (4-9.5 micron), and the bending stiffness depends by the square of the diameter. UHMWPE fibrils and fibers have only weak bonds that join them together because the PE is an apolar material. Apolar material means that electrostatic forces that join fiber together are weak, and also the interaction with the matrix is weak.

Moreover, the interaction of Dyneema and the matrix is not very predictable: probably the gluing points, given the non-polar nature of the fibers, are concentrated where there is some imperfection on fibers or where the EVA matrix is able to penetrate between one fiber and another one.

So, when a sample is bent for the first time, the Dyneema layer gets deformed, buckling starts to occur (also in the filament and fibers) and some of the weaker bonding points probably break. This explains why the sample decreases its stiffness after the first bending. When we bend the sample 10 times, many bonding points break, and the buckling occurs for small loads. if there are fewer constraints, less bonding point, the buckling tension decreases). After ten bending cycles, the buckling tension is so low that the stiffness of the sample is like a sample without the flexible skin, as the FEM simulation shows.

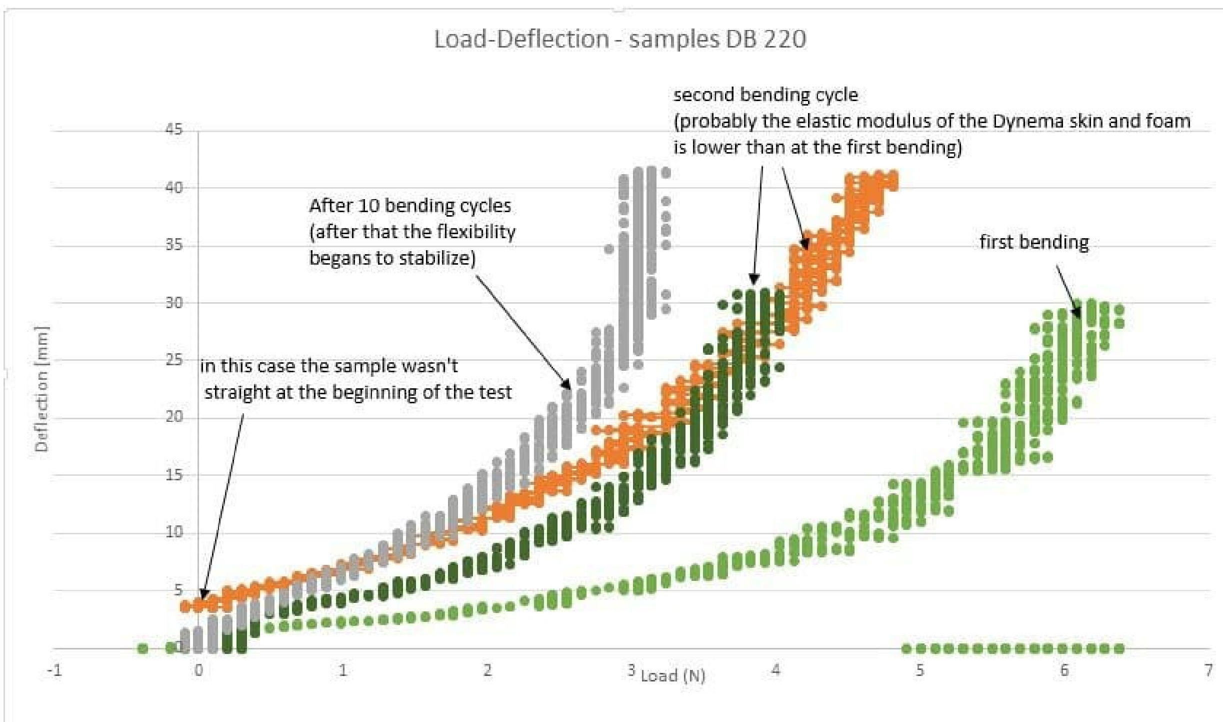

Figure 4.8 load-deflection graph of a Madflex on flexible side

4.7.2 Comparison of FEM and Experimental Results

According to the previous section, we could find out the behavior of the flexible side of Madflex changes as the number of load cycles increased, and these changes are related to Dyneema behavior. Thus, we can have a precise comparison between FEM analysis and experimental data if we consider Dyneema face properties different for the first cycle and following cycle of loading.

Therefore, for the first cycle of loading, we have considered the Dyneema Elastic modulus 500Mpa and in the following cycles, we have considered it near to zero. So, we can see in fig 4.9 a good consistency between FEM analysis and experimental data even in the first cycle.

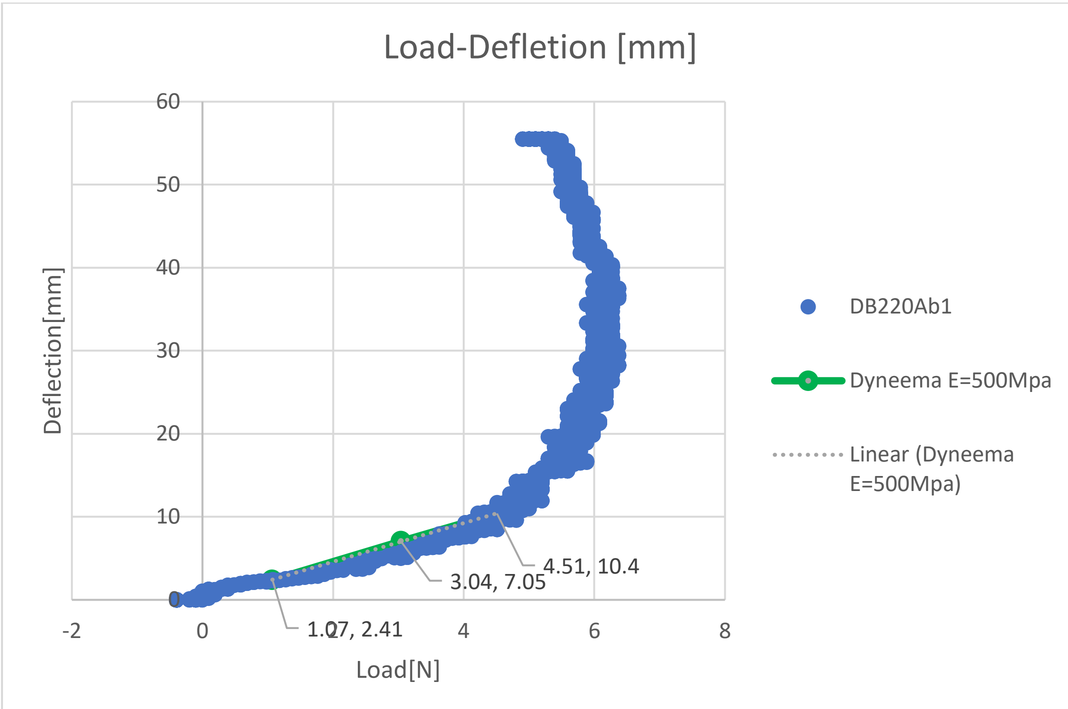

Figure 4.9 Load-Deflection of FEM and sample DB220Ab1

5. Aerodynamic Application of Madflex in Car Spoiler

5.1 Introduction to Automotive Aerodynamics

Nowadays, the aerodynamic of the automobile is a critical concern of body design particularly in the field of racing car in which the consideration of performance gain can be essential and in some categories such as F1 that the high-rank teams spend a major of budget to find aerodynamic efficient solutions against their competitors.

In this chapter, we discuss about loads generated by aerodynamic features that are mainly generated during acceleration, braking and cornering and transmitted through the tires to the ground hence the reaction of these forces to the grand through the four wheels shows us the advantages of aerodynamic performances on the car.

Vehicle potential cornering depends on some parameters such as suspension set up or vehicle tires cornering potential but if the vehicle is designed with a good base set up of suspension and also toe and camber setting then the only way to increase the cornering performance is considering good aerodynamics feature to create more downforce on the car.

Therefore, the necessity of aerodynamics design of vehicles makes sense why some companies emphasis to optimize aerodynamic features and spend more budget on this field of engineering and they are inducing new technologies in this field.

5.1.1 The effects of main aerodynamic forces

There are two main forces that have effective results on a vehicle aerodynamic performance, and these are Lift and Drag. The Lift force defines the force on the vehicle which is separating the vehicle from the road by applying pressure around the car, so we need a negative lift force in the case of automotive and we call it downforce. As we described before Downforce increase the vertical load on the tires so it can increase the ability of the vehicle to be more efficient in the corners.

An efficient way to increase downforce is by increasing the vertical load on the tires by adding mass on the vehicle, but it makes the vehicle slow in case of accelerating or braking.

By adding aerodynamic downforce force, we can increase the performance of the vehicle by increasing the efficiency of other parts.

The other main force is Drag; the Drag force is an aerodynamic force that applied against the direction of the vehicle moving. This force generated by pressure around the vehicle body. Drag effects the acceleration of vehicles and is a critical force at high speed.

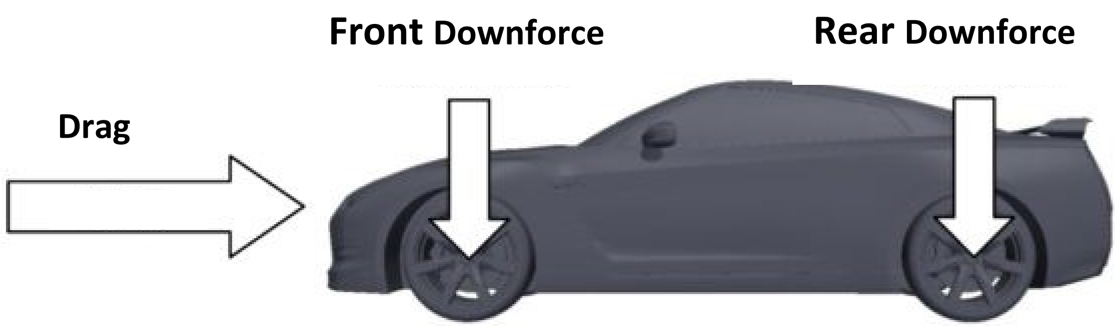

Figure 5.1 Drag and Downforce configuration on car

By increasing the aerodynamic downforce, we can speed up in the corners but also it leads to increase Drag. The optimized aerodynamic of a vehicle is always a trade-off with Drag and downforce. To increase the aerodynamic of a vehicle we need to increase downforce and decrease Drag. The goal of efficient aerodynamic is to increase the downforce as possible with little increase in drag thus we can increase the overall aerodynamic efficiency.

This goal is reached by designing different aerodynamic features on the car body such as Front Splitters, Canards, Rear Diffusers, Rear Wings, etc.

5.1.2 Drag

Drag force is an aerodynamic force that applied against the direction of the vehicle moving. Drag is directly proportional to the relative movement through the air and solid object.

Drag is generated by the friction of the surface of a solid body and air molecules in a boundary layer. Thus, Drag depend on object and fluid properties. The roughness of the solid surface and viscus force during the movement of air and Reynold number all effect on the Drag force.

Another form of Drag so-called interference Drag that is created by a change of direction of fluid flow around the body the creation of vortex. A vortex zone is a zone that the molecules of the air have spinning motion. Therefore, the shape of the solid has a direct effect on Drag.

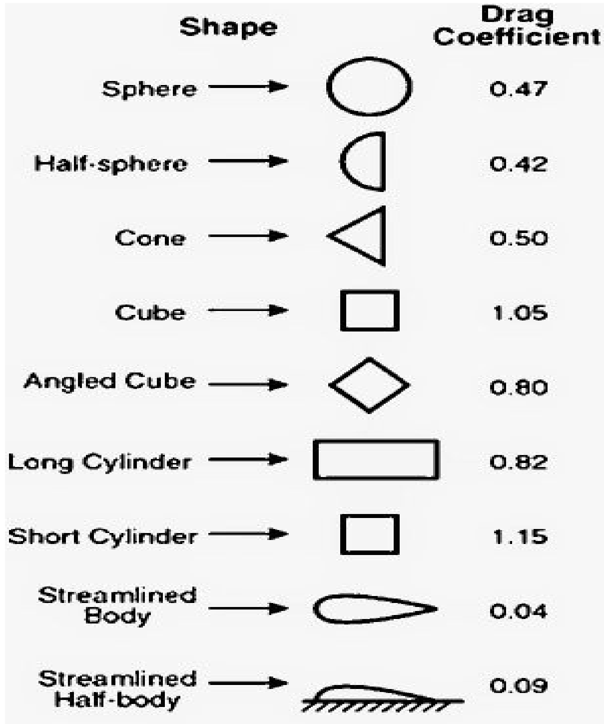

Figure 5.2 Drag coefficient of different shape

Thus, the Drag induce by a coefficient which is defined according to the shape of vehicle. The Drag force can be calculated by the formula bellow.

$$F_d = \frac{1}{2}\rho v^2 A C_d \qquad (5.1)$$

Where

F_d	Drag Force
ρ	Air Density
v^2	Relative speed of the solid and air
A	Reference Surface Area
C_d	Drag Coefficient

5.1.3 Downforce

According to Isaac Newton law, the total energy is constant in a close system, and this can be converted from one form to another form of energy, and then the total energy in a steady flowing fluid was formulated by Daniel Bernoulli.

According to the Bernoulli law, the pressure of the fluid is decreased by increasing the speed of the fluid and an aerodynamic force creates around a body by varying the pressure difference around that

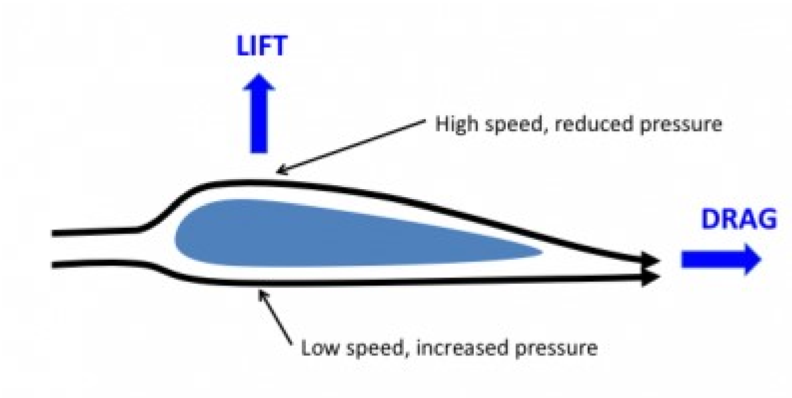

Figure 5.3 Pressure difference around airfoil

The Spoilers in car body follow Bernoulli law by the airfoil shape, the air-fluid speed up in one face of a spoiler so the aerodynamic pressure decrease and the pressure difference in another side of spoiler make aerodynamic force which according to the airfoil shape of spoiler it can be a positive so-called lift or negative as downforce in which in-car aerodynamics it designs how to generate downforce.

5.1.4 Laminar and turbulent flows

When a solid shape moves inside of a steady-state fluid like air, makes some movements in the fluid molecules and disturbs them. If the air molecules move in a parallel line so this flow known as laminar flow and on the contrary if the molecules of air move disordered and opposite to each other, so this kind of flow known as turbulent flow.

The kind of flows that follow the car body as a laminar or turbulent change the drag coefficient dramatically so according to an aerodynamic point of view it's so much important to manage the airflow around the car body.

The spoilers play a critical role to change the streamlines and make some turbulent around the body and lead to generate the downforce.

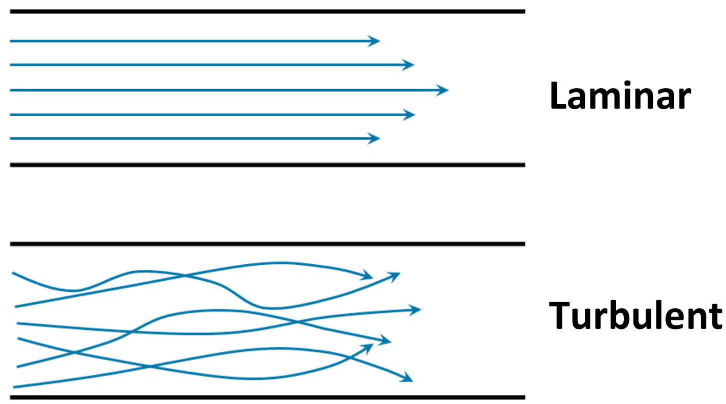

Figure 5.4 Laminar and Turbulent flows

5.2 Airfoil Shape Process

The Airfoil is a wing shape solid with a cross-section that can generate an optimum pressure disputation in each side of that and makes different pressure distribution on the top and bottom face of the airfoil.

A typical airfoil section is illustrated in the below figure, different geometric parameters as shown in the figure affect airfoil specification. The airfoil is symmetric if the mean camber line be straight and otherwise it's a cambered airfoil.

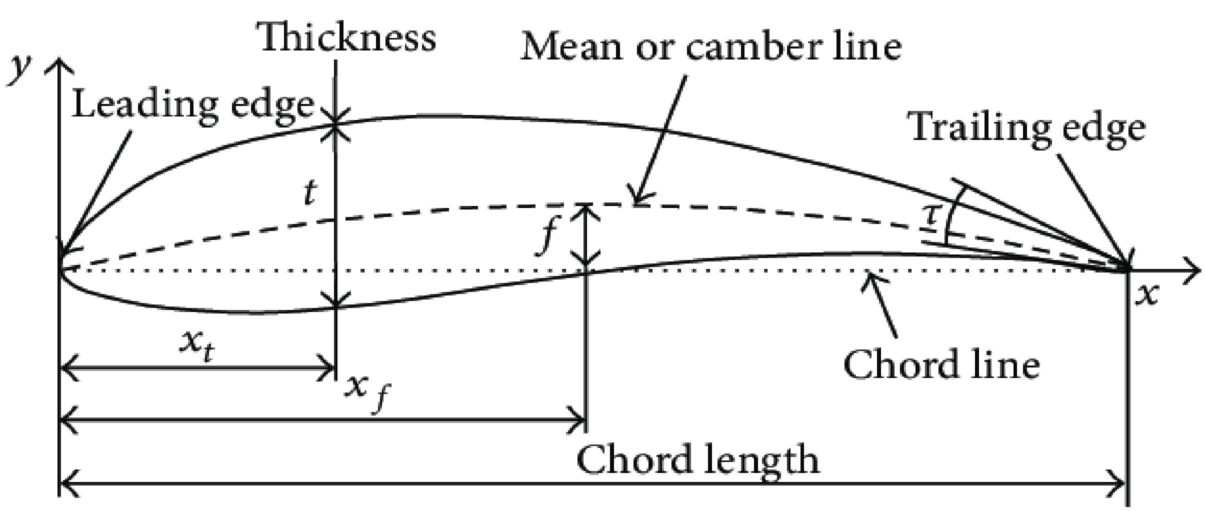

Figure 5.5 airfoil shape

The force created by the airfoil shape can be calculated by multiplying the total pressure by the area that is applying. The total force created by an airfoil is a function of different parameters such as the geometry of the airfoil, angle of attack, airspeed. An efficient airfoil design such as the drag stays in a minimum amount and then generating the maximum of downforce.

5.3 Spoiler

The spoilers are the airfoil shape devices that usually install in the front and rear of cars particularly in racing cars, this wing shape device installs in the back of the car to generate desired downforce and it leads to sticking the tires to the road so the performance of car increase and it will be more stable actually in case of cornering and braking.

In some cases, a spoiler installs on the back of the car just to make the style of the car better and little effect on aerodynamic forces

Obviously, we can calculate the force around the car by consideration of some properties of air around the car such as density, temperature, velocity, and pressure more over the consideration of the geometrical properties of the spoiler.

5.4 Active aerodynamic and spoilers

The spoilers are designed to creating favor downforce by disturbing the airflow around the car which is in a stable direction and situation, but the situations of driving and road are not the same as usual.

We can consider a racing car that is designed to have high performance in the cornering then the criterion of designing the spoiler is maximum disturbing airflow at the sharp edges, this situation is not so efficient when this car is speeding up in a streamline direction, to speed up we have to minimize the drag and minimize the aerodynamic resistance. So as usual particularly in the racing car, we need to change the spoiler geometry for the different conditions of driving.

In an active spoiler, the position and angle of attack can be changed to speed up and cornering by some mechanical instruments like hinge and actuators.

Moreover, in the braking situations, the active system of the spoiler can be automatically or manually changing its situation and increase the handling and stability of the car.

As a result, an automated spoiler that can be changed by some actuators to increase the performance of the car is quite efficient.

5.5 Formula SAE and Polytechnic of Turin Racing team (SquadraCorse)

Formula SAE is a competition organized by the Society of Automotive Engineers with the aim of inspiring students to design, build and develop a single seater prototype and make it race against other universities' teams.
The main goal of the competition is to spread out the “learn by doing” attitude and to prepare students to face the working environment immediately after the graduation. The competition takes place all over the world in the most important motorsport circuits and an overall ranking is made on the base of the single events results.

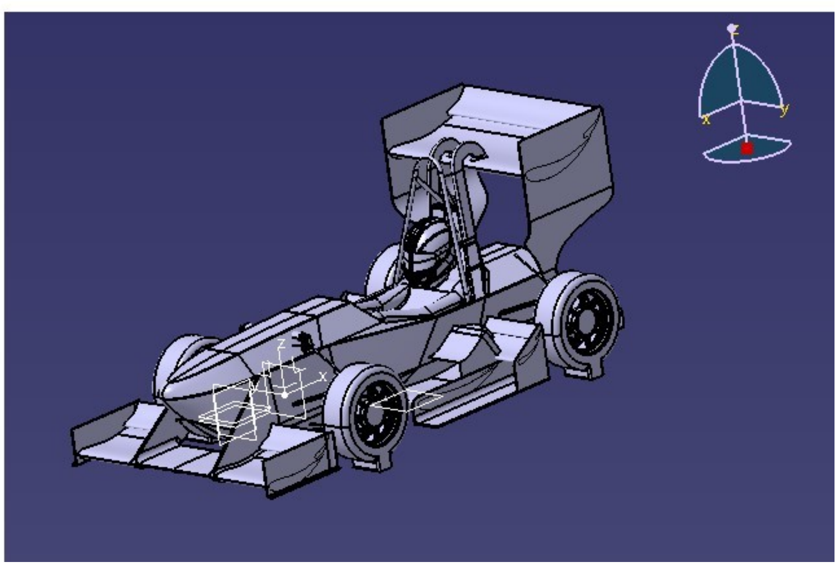

Figure 5.6 Formula SAE CAD model

The SquadraCorse was born in 2005 from the initiative of ten motor vehicle engineering students, united by the passion for car racing and in particular by designing and building a racing car prototype.

The first SC was born from this idea: a racing red livery, in homage to the automotive history of Italy such as the great Alfa Romeo, Ferrari, and Maserati manufacturers, and the number 46 on the nose, to pay homage to the celluloid idol Cole Trickle, played by Tom Cruise, and protagonist of the movie "Days of thunder", Tony Scott's film, particularly loved by the guys of the team.

5.6 Application of Madflex on Politecnico SAE team

The intelligent interaction of the active aerodynamic elements guarantees the optimal combination of downforce and low air resistance. The system reacts to the respective driving situation and the vehicle settings selected by the driver and accordingly varies the position of the rear spoiler to the calculated optimum.

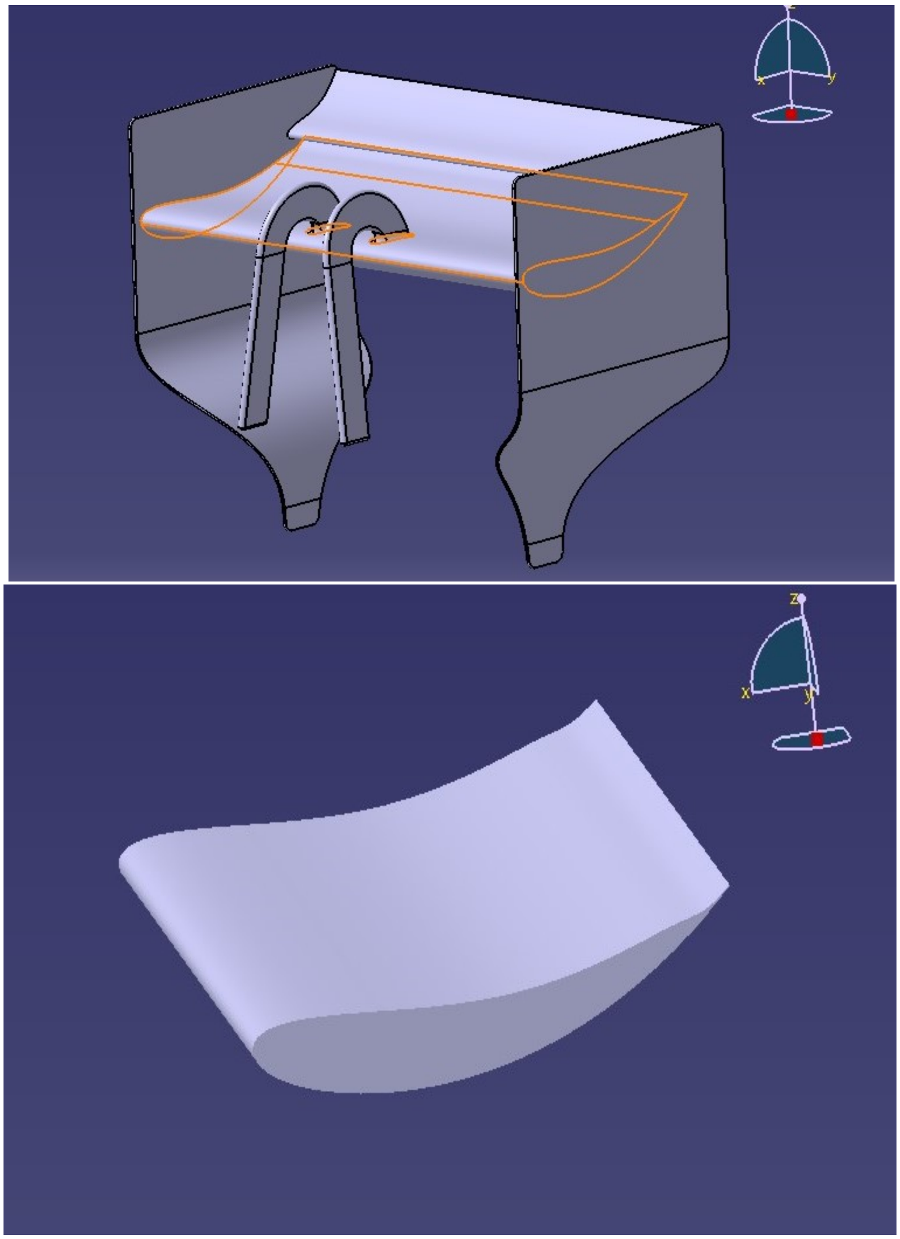

Figure 5.7 Formula SAE CAD model of spoiler

The concept of active rear spoiler (wing) for the Polytechnic of Turin SAE team started by applying the Madflex sandwich to the rear wing illustrated in the figure. The rear wing changes its position depending on the driving situation. The control software takes numerous parameters into account: It evaluates the driving speed and lateral acceleration, and the rear wing reacts to the situation then the airfoil shape changes to the optimum form and it can be also be applied by manually switch.

The spoiler assumes different heights in order to either optimize driving stability or reduce air resistance or increase the top speed. If the system detects transverse dynamics, the spoiler moves to the steepest dynamic position, thus guaranteeing both dynamic and safe driving behavior.

The combination of flexibility and stiffness of the MadFlex, coupled with its lightness, enable the development of aerodynamic elements capable of adapting their shape to different conditions, with possible applications not only in the field of sport racing, but in the entire automotive sector.

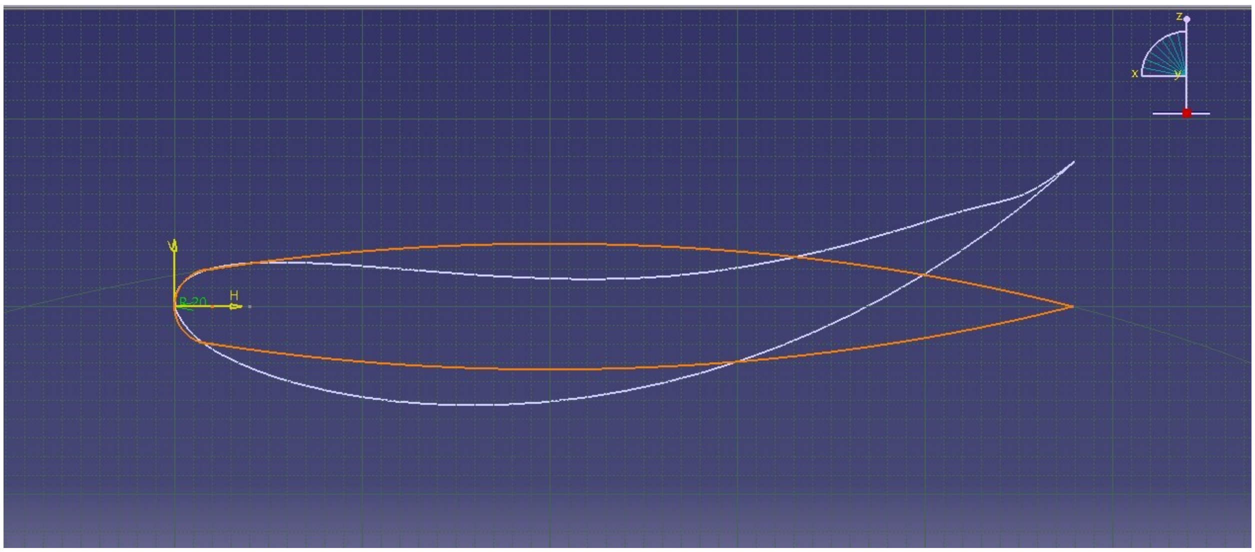

Figure 5.8 Formula SAE CAD model of spoiler shape changes

According to the figure the top and down of the main wing in the rear of the car can be manufactured by Madflex then it can bend to the top to reach the rigid situation and then the maximum downforce can be applied on the wing and so it can increase the car aerodynamic performance to the optimum point.

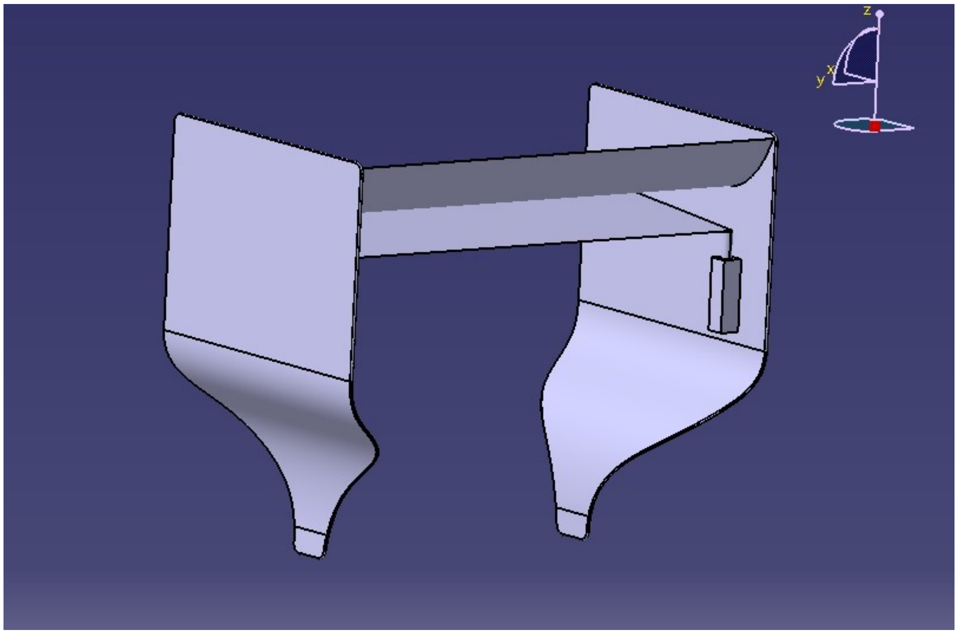

Figure 5.9 spoiler shape changes by electrical actuators

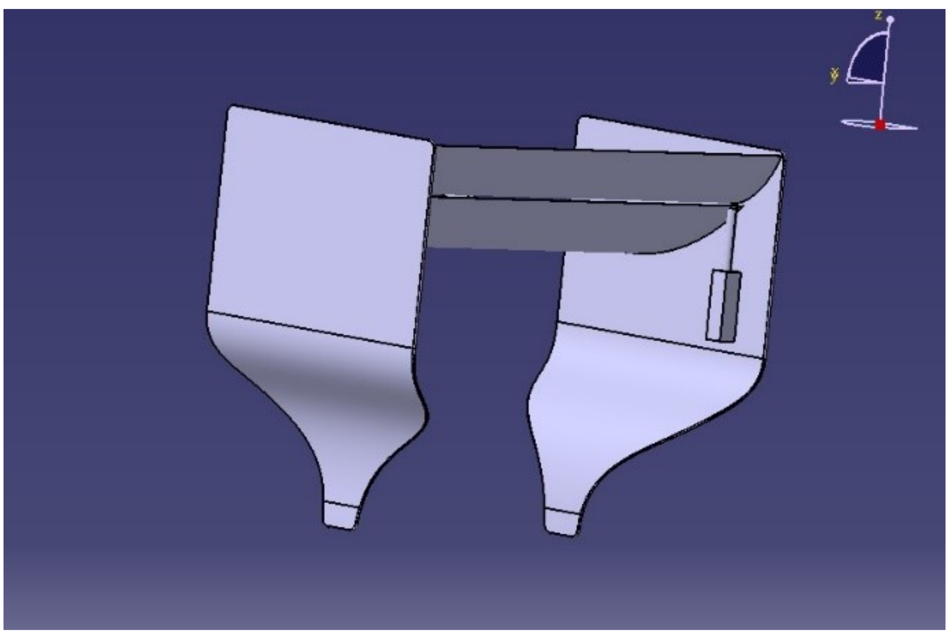

Figure 5.10 spoiler shape changes by electrical actuators

The concept can be applied by using two pneumatic or electrical actuators which mounted on both sides of the main rear wing. These actuators can change the shape of the wing by vertical movements to reach the maximum downforce by the rigid face of Madflex .

According to the figures, Its apparently visible that the main wing can be fixed to the minimum drug coefficient shape when the actuator is in the bellow, and when it actives and the lever of the actuator does to the top, the main wing shape change to the best efficiency of the airfoil shape.

5.7 Spoiler Manufacturing

The MadFlex can be employed in different ways to produce a deformable spoiler.

The simplest solution is creating a MadFlex hinge integrated in a standard composite sandwich panel. In this case the leading edge and the trailing edge of the spoiler made of a standard sandwich and a MadFlex central section of the spoiler will allow bending in order to increase or to decrease the camber of the airfoil. The MaFlex allow also to set a maximum deflection of the trailing edge, and then the maximum/minimum camber.

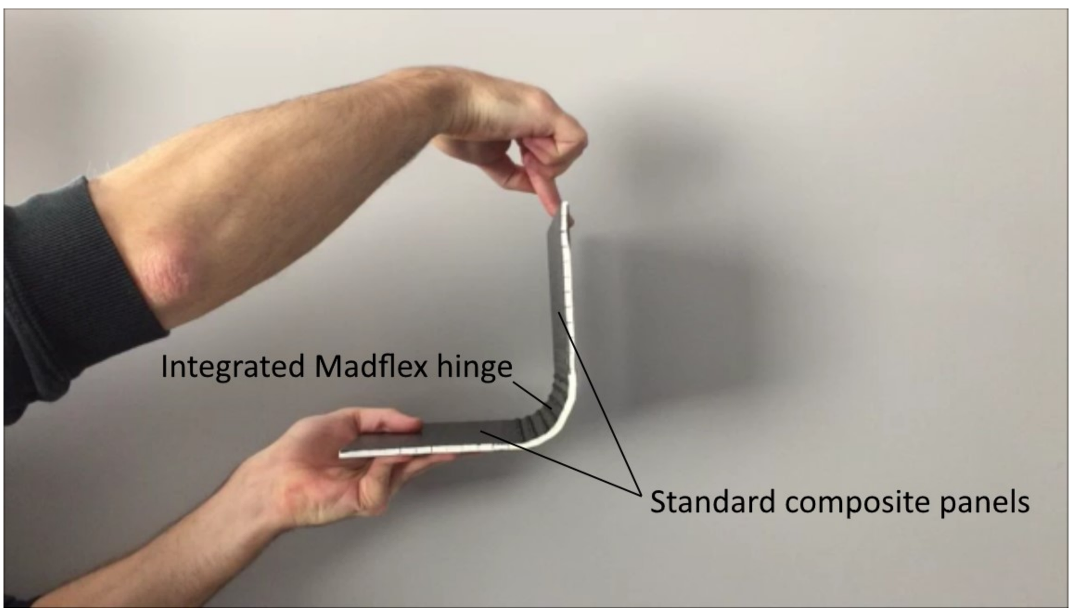

Figure 5.11 Integrated Madflex hinge

In the described example, the leading edge can be fixed to the car chassis and the leading edge to an actuator that regulates the camber.

Also a passive actuation is possible: in that case the camber will be regulated by the balance of aerodynamics forces and elastic forces of MadFlex (the force that the asymmetrical sandwich need to be bended). Further a spring or a elastomeric device can be added to regulate the relation between aerodynamic force applied and deflection.

The size of the hinge may vary according to requirements. The width can be a fraction of the Airfoil chord, or, in the extreme case, it can be equal to the chord: in the second option the whole spoiler is made using MadFlex.

In order to produce the described solution, a polymeric foam block can be milled into the spoiler shape, in order to create the core of the spoiler. Some slots will be milled on the surface where the integrated MadFlex hinge is desired. A mould for the dorsal surface of the spoiler is also made. In the production process, the carbon fiber pre-preg layers are placed on the mould (the mould should be first coated with a release agent); then the milled foam core is placed on the carbon layer. Then, the other skins are placed on the upper surface of the core: carbon pre-preg is placed where the sandwich must be stiff, and a patch of UHMWPE fabric is applied where the sandwich must be flexible. In order to join the UHMWPE patch on the core, a glue layer is interposed between the fabric and the foam. The mould and the other layers are then covered using a peel ply, a breather layer and a bagging film. In other words, the standard vacuum bagging technology is applied.

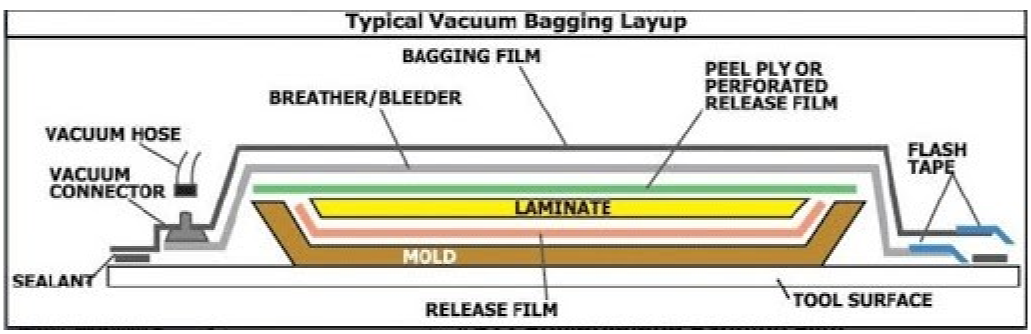

Figure 5.12 Madflex vacuum mold

Then the vacuum is created inside the bag, and the mould in putted inside the autoclave for the curing process.

5.8 FEM Analysis

In this section, we are going to simulate a plane model of Madflex that can be either used as a hinge in a specific part of the spoiler to change the airfoil shape or also can be used in the upper a lower face of the spoiler.

The concept is exactly as stated in the previous part and is illustrated in figure 5.11 therefore a plane model of Madflex is simulated that consist of two parts, the left side of that is manufactured as a standard sandwich but the right side is a Madflex that play a role as a hinge which can be used as a part of the upper and lower face of the spoiler that is used in the SAE formula car so all the dimension of FEM simulates is consistence to the real spoiler in the car and the material properties and configuration are exactly the same as the one that used in the FEM analysis in chapter 4.

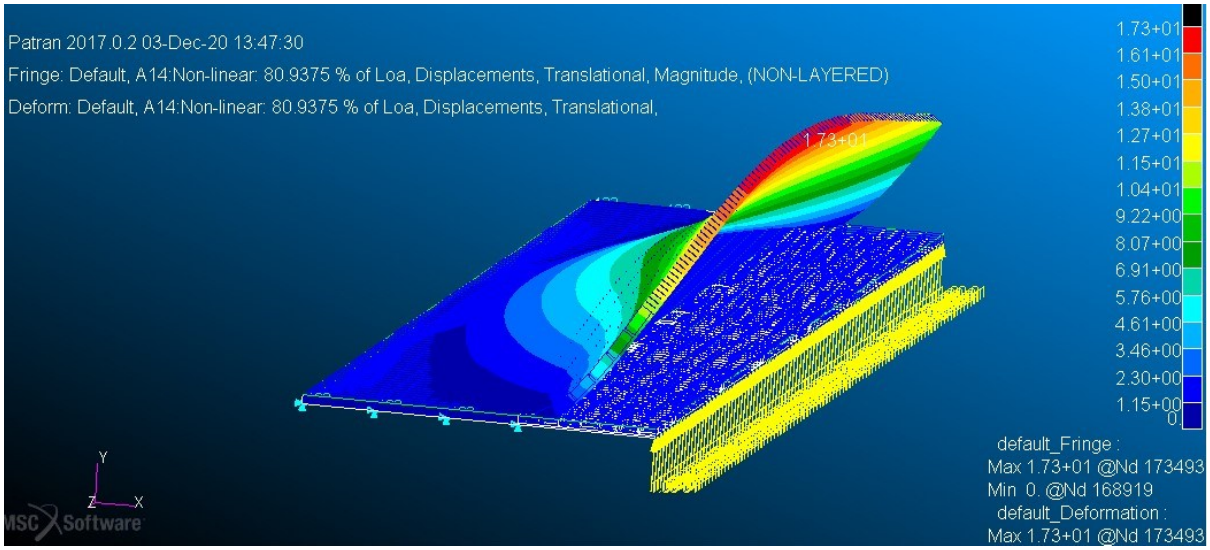

Figure 5.13 FEM Analysis of Madflex hinge

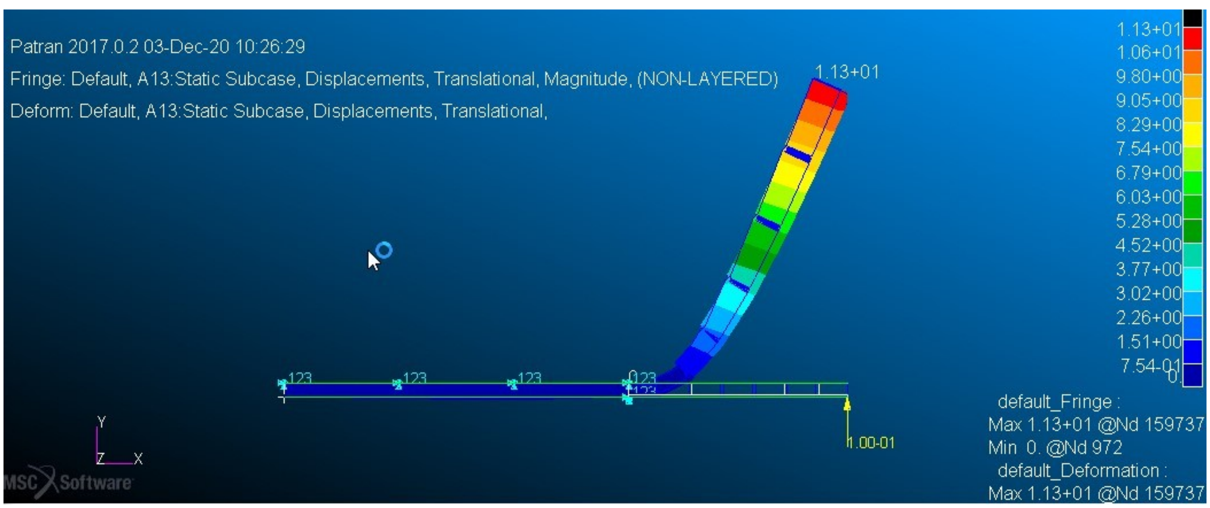

Figure 5.14 FEM Analysis of Madflex hinge

5.9 Boundary Conditions

By considering the airfoil shape of the main rear spoiler in the SAE car, it’s possible to constrain the lateral side of the spoiler to the vertical walls, so as it is shown in figure 5.13 the ends of the simple sandwich part are fixed in three directions of x,y,z. that is defined in

Patran as <0,0,0>. And a distributed force is applied in the lateral edge of the spoiler that is manufactured as a Madflex.

The boundary conditions of the simulated model are changed according to figure 5.14 In this configuration not only the lateral side of the spoiler is fixed in three directions but also the hinge section of the simple sandwich form is fixed in three directions of x,y,z, like <0,0,0>.

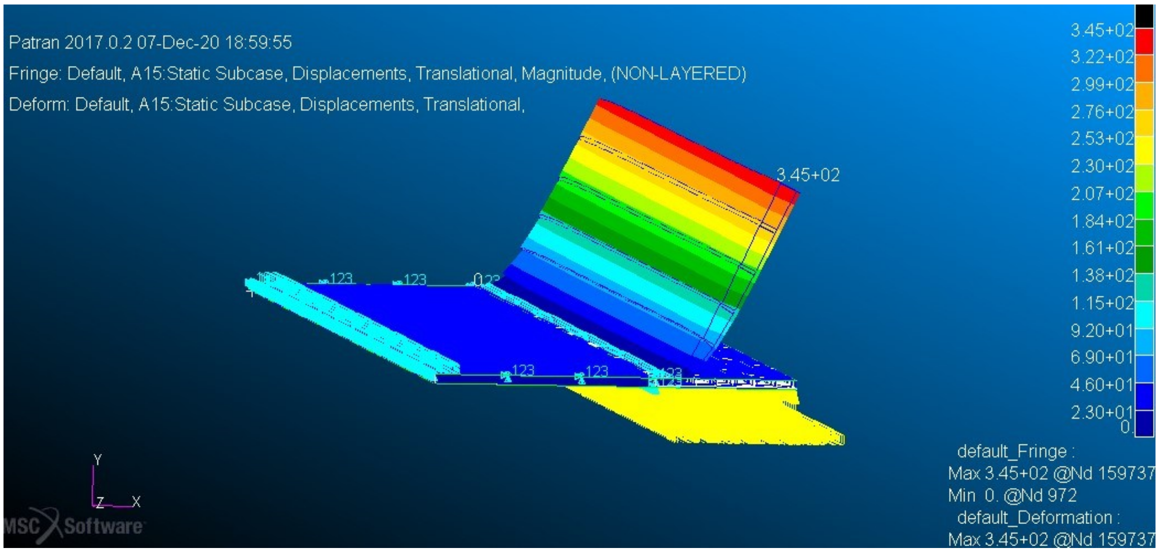

Figure 5.15 FEM Analysis of Madflex hinge

According to the CFD analysis that performed by the Formula SAE team, the maximum downforce created at the speed of 60 Kph is equal to 1200 N, so in this situation, it's considered that this maximum downforce is applied on the flexible side of the spoiler as a distributed force and the standard sandwich configuration that is constructed on the fixed part of spoiler is constrained around this fixed part, thus the fix part of spoiler boundary conditions are zero displacements along the x,y,z directions as <0,0,0> and the distributed downforce is applied as <0,1200,0> along the y-direction. As is illustrated in the figure 5.16 in the real one the maximum displacement of the Madflex part of the spoiler according to this configuration is equal to 345 mm.

Conclusion

In this thesis, the research was performed base on Madflex, a new technology in the field of sandwich materials which is patented by Composite Research Co. (CoRe).

The innovative advantage of this material is the possibility of being flexible, even rollable in one specific direction and in the opposite side, it is totally rigid.

Some experimental bending tests were performed on Madflex according to ASTM D7250/D7250M Standard. Simultaneously, the FEM simulation of the test was modeled by PATRAN & NASTRAN, with some modification on FEM model applied by computing, the experimental and FEM model results show to have the best consistency between the real test and the FEM analysis.

Madflex can be used in a wide range of applications in industrials such as automotive, aerospace, etc. Thus, in the second section of the thesis, the feasibility of the Madflex application was performed on the rear spoiler of the car. This part was done by collaborating with the Formula SAE and Polytechnic of Turin Racing team (SquadraCorse), and all the CAD design of the spoiler and the racing car performed by CATIA.

The combination of flexibility and stiffness of the MadFlex, coupled with its lightness enabled Madflex to change its position depending on the driving situation and produce maximum downforce in a very efficient way thanks to changing the shape of the airfoil manufactured with Madflex.

REFERENCES

[1] Allen H.G., Analysis and Design of Structural Sandwich Panels, Pergamon Press, Oxford, 1969.

[2] Plantema F.J., Sandwich Construction, John Wiley & Sons, New York, 1966

[3] Abbot, H. I. & Doenhoff, A. E. V., 1959. *Theory of Wing Section.* New York: Dover Publications, Inc.

[4] THE HANDBOOK OF SANDWICH CONSTRUCTION Dan Zenkert, editor, 1997

[5] ASTM D7250/D7250M Standard Practice for Determining Sandwich Beam Flexural and Shear Stiffness

[6] Kasravi, n.d. Vehicle Aerodynamics. [Online] Available at <http://www.kasravi.com/cmu/tec452/aerodynamics/VehicleAero.htm >[Accessed 20 August 2014].

[7] Generalic, E., 2014. Laminar flow. [Online] Available at: <http://glossary.periodic.com[Accessed 18 July 2014].

[8] Glenn, E., 2014. The Physics Hypertextbook. [Online] Available at: <http://physics.info/drag/>[Accessed 27 June 2014].